Contents lists available at ScienceDirect

Water Research

journal homepage: www.elsevier.com/locate/watres

Molecular community data meets anaerobic digestion Model 1 (ADM1) – a study about the correlation between metagenome-centric metaproteomics data of a two-step full-scale anaerobic digester and its corresponding mathematical model

Patrick Hellwig [a,b,*], Ingolf Seick [c], Nicole Meinusch [a], Dirk Benndorf [a,b,d], Jürgen Wiese [c], Udo Reichl [a,b], Robert Heyer [e,f,*]

[a] Otto von Guericke University, Bioprocess Engineering, Universitätsplatz 2, 39106 Magdeburg, Germany
[b] Max Planck Institute for Dynamics of Complex Technical Systems, Bioprocess Engineering, Sandtorstraße 1, 39106 Magdeburg, Germany
[c] Urban Water Management/Wastewater, Hochschule Magdeburg-Stendal, Breitscheidstraße 2, 39114 Magdeburg, Germany
[d] Applied Biosciences and Process Engineering, Anhalt University of Applied Sciences, Microbiology, Bernburger Straße 55, 06354 Köthen, Germany
[e] Multidimensional Omics Analyses Group, Leibniz-Institut für Analytische Wissenschaften – ISAS – e.V., Bunsen-Kirchhoff-Straße 11, 44139 Dortmund, Germany
[f] Multidimensional Omics Analyses Group, Faculty of Technology, Bielefeld University, Universitätsstraße 25, 33615 Bielefeld, Germany

HIGHLIGHTS

- First integration of metagenome-centric metaproteomics with ADM1 modeling.
- 32–78 % of high-quality MAGs assigned to ADM1 trophic groups via grouping.
- Metaproteomics found trophic groups absent in ADM1, prompting data-driven model refinement.
- Protein-based MAG abundances were more variable than ADM1 parameter dynamics.

GRAPHICAL ABSTRACT

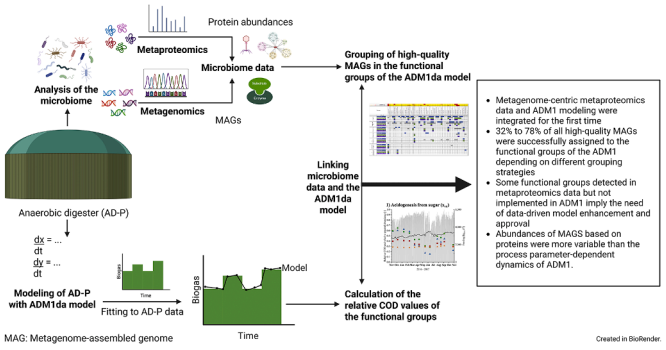

ARTICLE INFO

Keywords:
Anaerobic digestion model 1
Metaproteomics
Modeling

ABSTRACT

Advanced models, such as the Anaerobic Digestion Model No 1 (ADM1), are essential for operating, planning, and optimizing renewable energy production in anaerobic digester plants (AD-P)s. In this study, the ADM1da model was employed to simulate a two-step AD-P in an industrial setting. The ADM1da model is an extended ADM1 model for mixed substrates, accounting for substrate-specific disintegration, temperature effects, biogas-

Abbreviations: AD, Anaerobic digestion; AD-P, Anaerobic digester (plant); ADM1, Anaerobic Digestion Model Number 1; ADM1da, Anaerobic digestion model number one da (Extension of ADM1); BMP, Biomethane potential; COD, Chemical oxygen demand; fOTSrf, Degradable fraction of crude fiber; fRF, Fiber fraction of total solids; MAG, Metagenome-assembled genome; MPE, Mean percentage error; NH4-N, Ammonium-nitrogen concentration; ODE, Ordinary differential equation; OLR, Organic loading rate; RMSE, Root-mean-square error; t_{wm}, tons wet mass; VFA, Volatile fatty acids; TS, Total solids; VS, Volatile solids.

* Corresponding authors.
E-mail addresses: patrick.hellwig@ovgu.de (P. Hellwig), ingolf.seick@h2.de (I. Seick), dirk.benndorf@hs-anhalt.de (D. Benndorf), juergen.wiese@h2.de (J. Wiese), ureichl@mpi-magdeburg.mpg.de (U. Reichl), robert.heyer@ISAS.de, robert.heyer@uni-bielefeld.de (R. Heyer).

https://doi.org/10.1016/j.watres.2025.125272
Received 20 December 2024; Received in revised form 13 November 2025; Accepted 23 December 2025

Microbiome
Biogas plant
Anaerobic digestion
Anaerobic digester

related mass reduction, and mineral solids content. ADM1 models can represent the anaerobic digestion processes, although the biological assumptions are coarse and reflect the knowledge and available tools for microbial communities at the time of development. Meanwhile, metagenome-centric metaproteomics provides deeper insight into the metabolic activities of microbial communities in AD-Ps. Until now, this data has not been integrated with ADM1 models.

The objective of this study is to assess the feasibility of incorporating metagenome-centric metaproteome data into the ADM1 model. In a novel approach, 49 high-quality metagenome-assembled genomes (MAGs) with associated protein abundances were systematically classified into the trophic groups defined by the ADM1 model using specifically developed grouping rules. Abundances of MAGs were more variable than the process parameter-dependent dynamics of ADM1. Depending on the grouping rules, 32%-78% of all high-quality MAGs were successfully categorized into ADM1 trophic groups. However, some MAGs, e.g., *Methanotrix,* were multifunctional (acetoclastic and hydrogenotrophic methanogenesis) and required assignment to multiple groups. Unfortunately, more precise grouping rules resulted in greater discrepancies between metaproteomics data and the model. Additionally, 22% of the MAGs could not be assigned. The metagenome-centric metaproteome data imply that ADM1 probably needs extension to cover the observed microbial function of syntrophic acetate oxidizers, hydrolytic bacteria, lactate- and ethanol-fermenting bacteria, and mortality by phages. It was also observed that changes in process parameters, such as those caused by seasonal feeding, led to significant changes in the protein abundance

Integrating metagenome-centric metaproteomic data into ADM1 trophic groups was shown to be feasible. Some trophic groups detected in protein data but not implemented in ADM1 imply the need for data-driven model enhancement and approval. In the future, more accurate models considering molecular data could support a deeper understanding of microbial community dynamics in AD-Ps.

1. Introduction

The conversion of waste to biogas by complex microbiomes in anaerobic digestion (AD) is a key technology for renewable energy production. The microbiomes in anaerobic digesters (AD-P) consist of about 10–20 high-abundant (above 1 % of the microbial biomass/cell count) and partly redundant archaeal or bacterial key species and a multitude of further low-abundant species (Hassa et al., 2023; Heyer et al., 2024).

These microbiomes degrade the biomass in the four main steps: hydrolysis, acidogenesis, acetogenesis, and methanogenesis. The complexity of the microbiomes and the AD process is further complicated by two challenges. (i.) The microbiome and the AD process depend on parameters such as the feedstock, pH values, temperature, and AD-P design (Heyer et al., 2016; Maus et al., 2020; Rademacher et al., 2012; Vrieze et al., 2015; Zhang et al., 2014). (ii.) Within the microbiome, plenty of interactions between the different microbial species, including syntropy, competition, and phage-host interactions, exist (Heyer et al., 2019b; Orellana et al., 2019; Rossi et al., 2022). To keep an overview of the AD process and to have a powerful tool for operating, planning, and optimizing AD-P, reduced process models such as the Anaerobic Digestion Model 1 (ADM1) (Batstone et al., 2002) and its extensions, such as ADM1da (Karlsson, 2017; Ogurek et al., 2013), were developed.

The ADM1 is a mathematical model describing the physicochemical and biochemical processes (disintegration, hydrolysis, acidogenesis, acetogenesis, and methanogenesis) of the AD process and seven trophic microbial groups (Fig. 1). The ADM1 comprises ordinary differential equations (ODEs) and differential algebraic equations, covering 26 dynamic state concentration variables and 8 implicit algebraic variables per reactor vessel (Batstone et al., 2002).

Based on ADM1 and its adaptations (Mo et al., 2023), researchers investigated different fermenter settings (Bensmann et al., 2013; Blumensaat and Keller, 2005), dynamic processes (Bensmann et al., 2016), the potential of biological methanation (Bensmann et al., 2014), increased AD-P efficiency or integration of the AD process to complex biomass recycling (Meinusch et al., 2021; Seick et al., 2023). The abundance of microorganisms within the ADM1da based on the chemical oxygen demand (COD) is considered by assuming seven trophic groups of microorganisms conducting either (i.) sugar degradation ($x_{su,}$ acidogenesis from sugars), (ii.) amino acid degradation (x_{aa}, acidogenesis from amino acids), (iii.) long chain fatty acid degradation (x_{fa}, acetogenesis from long chain fatty acids), (iv.) valerate and butyrate degradation (x_{c4}, acetogenesis from butyrate and valerate), (v.) propionate degradation (x_{pro}, acetogenesis from propionate), (vi.) acetate degradation (x_{ac}, acetoclastic methanogenesis), and (vii.) hydrogen degradation (x_{h2}, hydrogenotrophic methanogenesis) (Fig. 1).

The used ADM1da of this study was created with the use of mixed substrates in mind and is thus also well suited for modeling agricultural AD-P (Ogurek et al., 2013; Seick et al., 2023). Compared to the original ADM1, this model variant can be used to better describe: characterization of different substrates due to different disintegration rates; temperature dependencies of the biological processes; mass and volume reduction in the fermentation substrate according to biogas production; Total solid (TS) concentrations due to the integration of a mineralic fraction in the model. A significant distinction of the ADM1da model from the fundamental ADM1 model is the capacity to differentiate between slowly and rapidly degradable feedstocks (composites) for the disintegration process, with this differentiation being made separately for carbohydrates, proteins, and fats.

Despite all the previous research studies (e.g., 272 publications found under the term "ADM1" on PubMed, 18 September 2024), there are still weaknesses in the model requiring further improvement. For example, hydrolysis is assumed to be a rate-limiting step, but it is debated whether it should be described by simple first-order kinetics or by the inclusion of the biomass of hydrolyzing microorganisms using a Contois kinetic (Contois, 1959; Wang and Li, 2014). This is due to a paucity of data regarding the production and degradation of extracellular hydrolases. Furthermore, a paucity of detailed information exists regarding the decay of microbial species by, for example, phages and microbial effectors (Heyer et al., 2025; Krysiak-Baltyn et al., 2017). It is recognized that important microbial groups that are essential for the AD are missing from the current model and should be considered for model refinement. In particular, hydrolyzing bacteria (Normak et al., 2015), syntrophic acetate oxidizing bacteria (Rivera-Salvador et al., 2014), lactate fermenting bacteria (Du et al., 2025), and ethanol fermenting bacteria (Satpathy et al., 2016) are not included in the present ADM1 model. However, recent microbiome studies of full-scale and lab-scale biogas reactors have consistently demonstrated the presence and significance of these microbial groups in the anaerobic digestion process (Harirchi et al., 2022).

Hydrolyzing bacteria such as *Clostridium, Ruminococcus, Ruminofilibacter, Acetivibrio, Butyrivibrio, Halocella, Eubacterium, Bacteriodes, Bacteriodites, Spirochaeta, Thermotoga*, and *Petrotoga* have been identified as essential for subsequent biogas production steps, as they initiate the degradation of complex biomass (Azman et al., 2015; Cirne et al., 2007). Syntrophic acetate oxidizing bacteria, such as members of

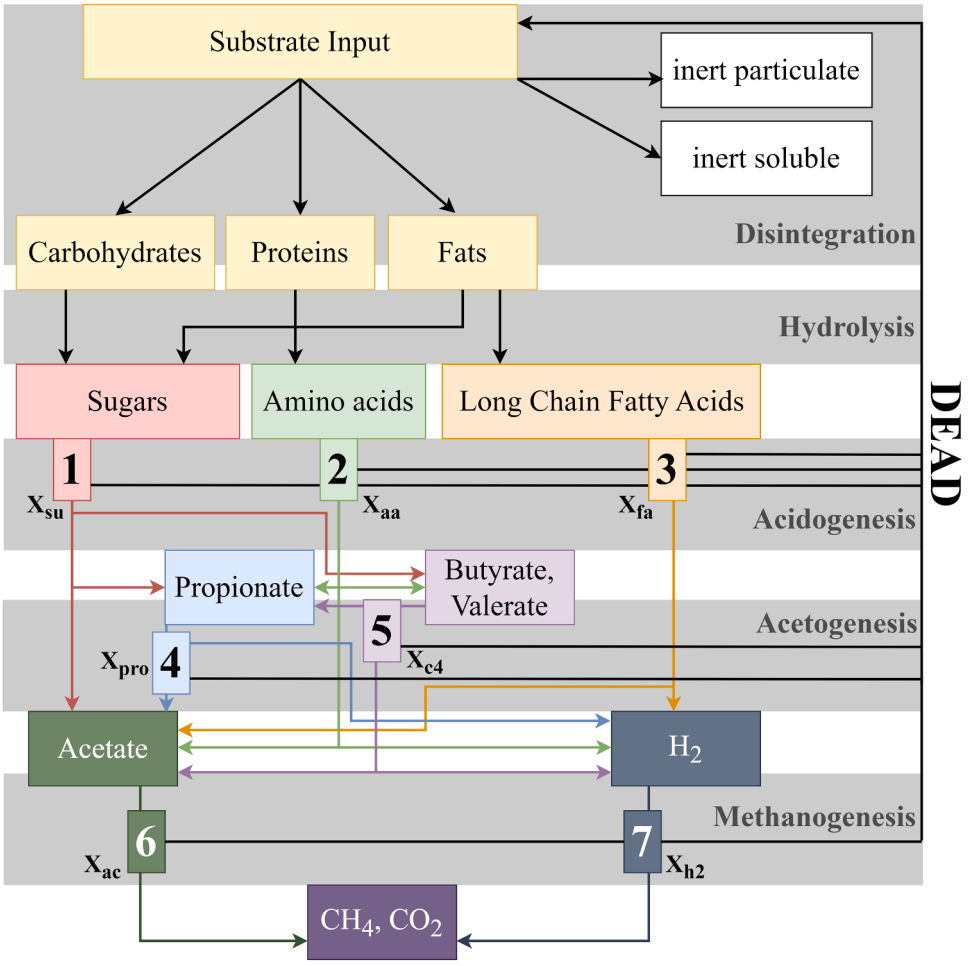

Fig. 1. Biochemical processes of the ADM1da. (1) acidogenesis from sugars, (2) acidogenesis from amino acids, (3) acetogenesis from long chain fatty acids, (4) acetogenesis from propionate, (5) acetogenesis from butyrate and valerate, (6) acetoclastic methanogenesis, and (7) hydrogenotrophic methanogenesis. Modified from Karlsson (2017) and Batstone et al. (2002). x_{su}: sugar degraders, x_{aa}: amino acid degraders, x_{fa}: fatty acid degraders, x_{c4}: valerate and butyrate degraders, x_{pro}: propionate degraders, x_{ac}: acetoclastic methanogens, x_{h2}: hydrogenotrophic methanogens.

Dethiobacteraceae, Syntrophaceticus, Tepidanaerobacter, Clostridia, Thermacetogenium, and *Thermotoga*, have been identified under thermophilic and ammonia-rich conditions, indicating their crucial role in acetate conversion (Dyksma et al., 2020; Mosbæk et al., 2016). Similarly, lactate-fermenting bacteria, including *Lactobacillus, Clostridia, Aeriscardovia, Halanaerobiales, Fusobacteriales, Thermotogales*, and *Thermoanaerobacteriales* have been detected (Akinsola et al., 2025; Detman et al., 2018; Moestedt et al., 2020). Ethanol-fermenting bacteria such as members of *Firmicutes, Caloramator, Clostridium, Herbinix, Defluviitoga*, and *Halocella* have also been observed (Maus et al., 2016; Yang et al., 2022). These fermenting bacteria play an important role in direct interspecies electron transfer (Feng et al., 2021; Wang et al., 2026) and can lead to higher biogas production (Pipyn and Verstraete, 1981). One reason for these biological inaccuracies in the model has been the limited access to the underlying microbiomes for the collection of high-quality data that could be used for microbial modeling in ADM1.

Recent advancements in omics technologies, such as metagenomics (Campanaro et al., 2020) and metaproteomics (Heyer et al., 2015), provide new opportunities to investigate these microbiomes quantitatively. These technologies generate microbiome-specific high-quality data, which can be used for modeling and integrated with the ADM1 model (Basile et al., 2023; Heyer et al., 2019b). Whereas metagenomics has a better resolution, enabling the prediction of metagenome-assembled genomes (MAGs) (Bowers et al., 2017) and correlates better with the cell number, metaproteomics correlates better with biomass and metabolic function. Therefore, metagenome-centric metaproteomics enables the identification and quantification of the abundance of microbes and their metabolic functions. This, in turn, allows the assignment to the trophic groups of the ADM1da model. Applying this novel approach has the potential to identify important MAGs that were not considered in the current model. Our recent study (Heyer et al., 2024) provides comprehensive AD-P process data and metagenomic-centric metaproteomics data from an industrial-scale two-step AD-P over a full year.

For the first time, these data allow a comparison of the actual biomass composition and dynamics of the metagenome-centric metaproteome data with the biomass predictions from the ADM1da model over a one-year operating period. In particular, using data from the two-step digestion system (with two different process biological milieus) allows for a better comparison as well as better identification of discrepancies between the model and the metaprotein data.

To compare the metagenome-centric metaproteomics data (real biomass) with the predicted biomass from the ADM1da model, specific grouping rules were newly developed to systematically assign high-quality MAGs with their protein abundances to the trophic groups defined by the ADM1 model. The objectives are twofold: to ascertain the extent to which the ADM1da model's data aligns with the metagenomic-centric metaproteomics data, and to identify any discrepancies. The objective of this study is to ascertain the potential of metaproteomics in ADM1 modeling and to determine what can be learned from comparing

the ADM1 model and the metaprotein data. In particular, such discrepancies could show potential for future refinement of ADM1 using metagenome-centric metaproteomics, including the identification of missing trophic groups in the current ADM1 model.

2. Materials & methods

Besides the ADM1da model, this work is based on laboratory data already published in our earlier study. All information on the laboratory data can be found in Heyer et al. (2024). For this study, the process parameters (Supplementary Table 1) of the AD-P (Fig. 2) and the metagenome and metaproteome data were used.

2.1. Operation of the two-step anaerobic digester

The two-step AD-P comprised a hydrolysis fermenter, followed by a fermentation step consisting of a main fermenter and a secondary fermenter. These fermenters are operated as heated and continuously stirred tank reactors. The hydrolysis fermenter was a non-gas-tight reactor with a working volume of 200 m^3, while the main fermenter was a gas-tight reactor with a volume of 2100 m^3 for biomethanation (Fig. 2). The two fermenters are serially connected. Furthermore, a secondary fermenter (1030 m^3) was connected downstream of the main fermenter, from which material was pumped into the hydrolysis fermenter and mixed with the substrate. On average, the system was fed daily with 27.9 ± 2.6 tons wet mass (t_{wm}) of substrates, composed of 11.3 ± 1.2 m^3 liquid pig manure, 1.4 ± 0.7 m^3 liquid silage effluent, 0.3 ± 0.3 t_{wm} corn-cob mix, 13.3 ± 2.2 t_{wm} maize silage, and seasonally (October 2016 to March 2017), 1.5 ± 1.8 t_{wm} beet silage was also added. Furthermore, an average of 0.2 ± 0.3 m^3 solid fermentation residues was fed (a very small internal flow not considered in the model). The substrate was mixed with 49.2 ± 4.6 m^3 of liquid fermentation residues recirculated from the secondary fermenter (Supplementary Table 1). This substrate supply corresponded to an average organic loading rate of 40.0 ± 4.3 $kg_{VS} \cdot m^{-3} \cdot d^{-1}$ in the hydrolysis fermenter and 3.2 ± 0.5 $kg_{VS} \cdot m^{-3} \cdot d^{-1}$ in the main fermenter. Mean Hydraulic retention (incl. recirculation) times were 2.3 days in the hydrolysis fermenter and 24.0 days in the main fermenter. The mean retention times of substrates (without recirculation) were 7.2 days in the hydrolysis fermenter and 75.3 days in the main fermenter. The process temperature in the main fermenter was continuously monitored and maintained at 39.7 ± 0.2 °C. In contrast, temperature measurements in the hydrolysis fermenter were conducted during nine exemplary samplings, yielding an average of 39.9 ± 1.2 °C. Chemical analysis of reactor samples revealed a pH of 5.9 ± 0.4 in the hydrolysis fermenter and 7.9 ± 0.1 in the main fermenter. The ratio of total volatile fatty acids to total alkalinity was 3.3 ± 0.7 in the hydrolysis fermenter and 0.1 ± 0.02 in the main fermenter. Correspondingly, total acid concentrations were 14,380 ± 1980 $mg \cdot L^{-1}$ in the hydrolysis fermenter and 118.7 ± 154.5 $mg \cdot L^{-1}$ in the main fermenter. Total ammonia nitrogen in the main fermenter averaged 2340 ± 232 $mg \cdot kg^{-1}$ (data not available for the hydrolysis fermenter). TS content was 9.6 % ± 1.0 % in the hydrolysis fermenter and 5.8 % ± 0.7 % in the main

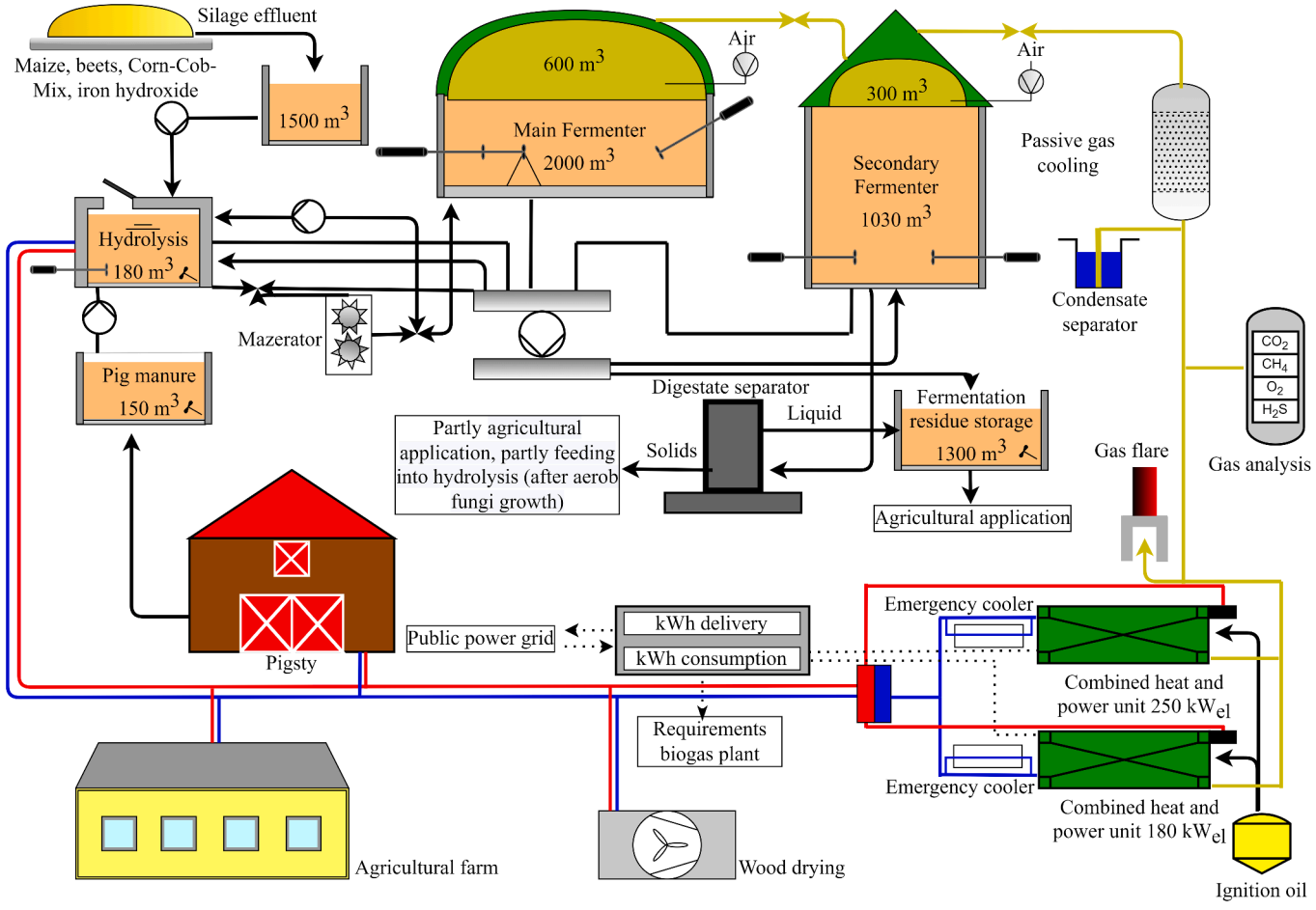

Fig. 2. Schematic representation of the two-step anaerobic digestion plant. The system includes a hydrolysis fermenter, a main fermenter, and a secondary fermenter (not analyzed in this study). On average, 77.3 ± 5.0 tons of wet substrate were fed daily into the hydrolysis reactor, mixed with 49.2 ± 4.6 m^3 of liquid fermentation residues from the secondary fermenter (Supplementary Table 1). Blue and red lines indicate heat flow, dotted lines represent electrical current, black lines show the movement of substrates or residues, and yellow lines depict the production of biogas. The original figure is derived from (Heyer et al., 2024).

fermenter. Volatile solids constituted 85.1 % ± 1.7 % of TS in the hydrolysis fermenter and 73.4 % ± 0.7 % of TS in the main fermenter. Average biogas production, measured only in the main fermenter, was 3170 ± 275 $Nm^3 \cdot d^{-1}$ with a methane content of 60.2 ± 1.5 vol % and a carbon dioxide content of 41.1 ± 2.5 vol %.

2.2. Representation of the AD process using SIMBA# and ADM1da

Simulations of the two-step AD-P were performed with the simulation software SIMBA# (Version 5.0) (Alex et al., 2013; ifak GmbH, 2021; Rojas et al., 2011) based on ADM1da (Karlsson, 2017; Ogurek et al., 2013). Additionally, a single-step process was simulated in the absence of a hydrolysis fermenter to facilitate a comparative analysis of two-step processes (Fig. 3).

The final SIMBA# model (ifak GmbH, 2021) of the two-step AD-P comprised seven pre-implemented building blocks: the biomass input/substrates (1), the converter blocks to calculate the ADM1da fractions from the substrate data (2), the hydrolysis block (3), the main fermenter block (4), the secondary fermenter block (6) the recirculation block (5), the gas analyzer block (7) and blocks for calculation of methane amount, methane yield and energy content of biogas (8) (Fig. 3). For the biomass input, the process parameters, and the AD-P design, we used the data provided by the plant operator (Supplementary Table 1), including the feeding, the temperature, and the fermenter sizes. Feeding information was forwarded to converter blocks of the SIMBA#, which are associated with a corresponding substrate model; the biomass input into a substrate composition utilized by the AMD1da (Supplementary Table 2).

For the input blocks of the simulation model, daily mean values of the measured feeding and recirculation amounts were used. According to the feeding of the plant during the one-year operational period considered in this study, the model input consists of pig manure, maize silage, sugar beet silage, corn-cob-mix, and silage leachate (Supplementary Figure 1). The TS of the substrates, Pig manure, Maize silage, and Sugar beet silage, were also given to the model as dynamic inputs according to the monthly laboratory measurements (Supplementary Figure 2). The concentrations of volatile solids (VS) and crude fiber (fRF) determined monthly on the same samples are assigned to the converter blocks of the modeled substrates after arithmetic averaging for each substrate as a constant parameter. For the final simulations, 365 days of lead time were simulated to adjust the system using constant settings (average values of feeding values), followed by 365 days of actual simulation matching to the actual analyzed period (described by daily values). To fit the simulation data to the actual AD-P data, the following three adaptations to the kinetic parameters of the SIMBA# implementations of ADM1da were made here, according to Seick et al. (2023): (i.) Increase of the upper limit for the modeled pH-limitation of methanogenesis (parameter $pH_{UL,ac}$ in process p11 in ADM1da from 7.0 to 8.5); (ii.) an increase of the half-saturation constants for NH_3 inhibition of propionic acid degradation and of acetoclastic methanogenesis (parameter $K_{INH3,pro}$ in process p10 in ADM1da from 0.0019 to 0.0025 $kmol_N\ m^{-3}$ and $KI_{NH3,ac}$ in process p11 in ADM1da from 0.0018 to 0.0025 $kmol_N\ m^{-3}$), (iii.) reduction of the acetoclastic methanogenic biomass decay rate (parameter $k_{dec,xac}$ in process p18 in ADM1da from 0.04 to 0.02 d^{-1}) (Supplementary Note Table S1).

Furthermore, and also according to Seick et al. (2023), the parameters of temperature dependencies of the disintegration and hydrolysis processes were increased. The factors in the exponents of the temperature functions (implemented in ADM1da) are increased from 0.024 to 0.069 for the parameters $k_{s,dis}$, $k_{f,dis}$ (slow and fast disintegration of composite) and $k_{hyd,ch}$ (hydrolysis rate of carbohydrates) as well from 0.024 to 0.055 for the parameters $k_{hyd,pr}$ (hydrolysis rate of proteins) and $k_{hyd,li}$ (hydrolysis rate of lipids). These modifications fit better with the Arrhenius equation approach, considering the reaction rate dependency on temperature, and are key to providing the required model fit (Supplementary Note Table S1).

These parameter changes are not a calibration for a specific case, but rather the application of suitable basic settings, which are recommended by Seick et al. (2023) as the basis for successful model adjustment.

As also described in Seick et al. (2023), the main part of the model adjustment was the setting of the inert fractions of VS from the substrates in the model so that the methane production of the plant was approximately achieved in the simulation. This inert fraction results indirectly from the parameterizations in the influent model by adjusting the parameters of biomethane potential (BMP), the crude fiber fraction of TS (fRF), and the degradable fraction of crude fiber (fOTSrf) in the substrate blocks of the respective substrates of the SIMBA# model (Fig. 3 and Supplementary Note Table S1).

2.3. ADM1da output data

To assess the model accuracy, we evaluated whether the exact representation of ADM1da fitted the actual amount of biogas and methane produced (Supplementary Table 3). The average simulated produced amount of biogas by the model was 3272 $m^3\ day^{-1}$ ± 203 $m^3\ day^{-1}$, and the measured biogas amount was 3176 $m^3\ day^{-1}$ ± 302 $m^3\ day^{-1}$

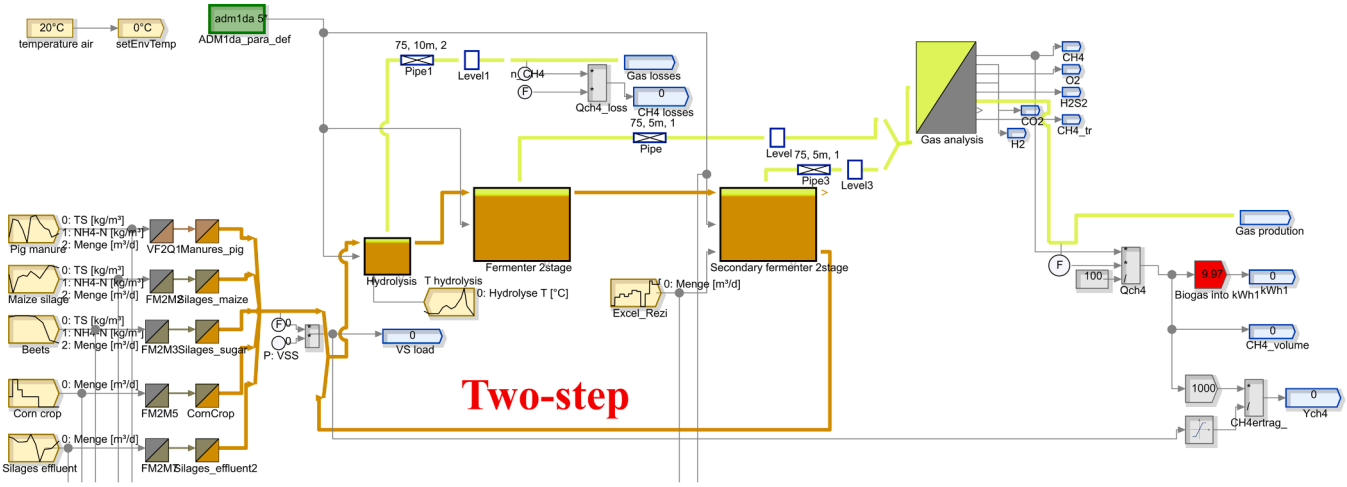

Fig. 3. Structure of the SIMBA# model used for simulations: 1. Biomass input, 2. Converter block, 3. Hydrolysis fermenter, 4. Main fermenter, 5. Recirculation of biomass, 6. Secondary fermenter, 7. Gas analyzer, and 8. Calculations (methane amount, methane yield, energy content of biogas). Brown lines correspond to biomass flow, green-yellow lines correspond to gas flow, and green lines correspond to control and measurement variables.

(Fig. 4A). Similar predicted methane content in biogas was 56 % ± 1 % compared to the measured 60 % ± 2 % (Fig. 4B), and the modeled produced methane amount was 1728 m^3 day^{-1} ± 105 m^3 day^{-1}, compared to the measured methane amount of 1911 m^3 day^{-1} ± 178 m^3 day^{-1} (Supplementary Figure 3 A).

Furthermore, the monthly laboratory analyses of the concentrations of TS, VS, and volatile fatty acids (VFA), pH values, and the ammonium-nitrogen concentration (NH4-N, only available for the main fermenter) were reproduced by the model in the operating year under consideration (Supplementary Table 2, Supplementary Figures 4 and 5). In particular, the simulated VS degradation can serve as a plausibility check for the correct simulation of gas production (Supplementary Figure 6). The comparison of the VS concentrations measured in the fermenters (VS_H: 82 kg m^{-3} ± 9 kg m^{-3}, VS_F: 42 kg m^{-3} ± 5 kg m^{-3}) with the monthly monitoring with the simulated time course (VS_{modelH}: 89 kg m^{-3} ± 5 kg m^{-3}, VS_{modelF}: 42 kg m^{-3} ± 4 kg m^{-3}) shows agreement.

2.4. Assigning MAGs to the trophic groups of the ADM1da

The protein abundances of microbial groups in the hydrolysis and the main fermenter were assessed by a metagenome-centric metaproteomics analysis covering twelve time points (Heyer et al., 2024). The performed metaproteomics analysis quantified the relative abundances of microbial groups based on the unique spectral abundance of identified protein groups. To compensate for measurement fluctuations between the mass spectrometry measurements and to make them better comparable, the spectral abundance of each protein group for each measurement was normalized to the total spectral abundance of each sample. The high-quality MAGs were grouped into the seven groups defined by the ADM1da model (see below). Given that only high-quality MAGs were utilized for the grouping, and these only reflect approximately half of the sample, they were normalized to 100 % between the trophic groups of the model. This ensured that they represent 100 % of the community and are comparable with the relative COD values of the model. The relative COD was calculated by means of normalization of the sum of all average COD values of the biomass over the course of the year. This normalization maintains consistency in the biomass dynamics of the predicted COD values. The relative COD values are then unitless, and they form the relative proportion of the COD distribution within the groups. Thus, these relative values can be compared with the relative protein abundances in each group. For the protein assignment to the microbial groups from ADM1da, the expressed proteins of high-abundant and high-quality MAGs (>90 % completeness, <5 % contamination) were first assigned to the 49 pathways relevant for the AD process (based on (Heyer et al., 2019a) and (Sikora et al., 2019)) using the MPA_Pathway_Tool (Walke et al., 2021). The mapping of the proteins from the MAGs to the AD process pathways was already done in our earlier study (Heyer et al., 2024), but we have also included the data in this supplement for better understanding (Supplement Mapping_data.zip). After the assignment of the proteins to the AD pathways, the pathway information was used for the assignment of the MAGs to the seven microbial groups (Fig. 1). The first rule groups the MAGs according to the ADM1da groups based on the metabolic functions from the literature associated with each MAG's taxonomy. MAGs with functions outside the seven groups of ADM1da or with low taxonomic resolution (below the family level) were excluded. This rule is referred to as the "Literature Rule " in the following. The second rule groups the MAGs based on the identified proteins associated with a pathway of ADM1da, without consideration of taxonomy. This rule is referred to as the "Pathway Presence Rule" in the following. The third rule, called "Extended Pathway Rule" builds on the "Pathway Presence Rule", incorporating specific thresholds and taxonomic information to categorize the MAGs within ADM1da groups. The final rule, termed the "Fine-Tuned Pathway Rule", represents an enhancement of the "Extended Pathway Rule". It incorporates additional ratios and protein abundance thresholds, thereby further refining the grouping. This is done to distinguish between sugar and amino acid-degrading bacteria and between primary and secondary fermenting bacteria (Tables 1 and 2; Supplementary Tables 4 and 5).

2.5. Mean percentage error, and spearman correlation

The mean percentage error (MPE) was used for the calculation of the deviations between the ADM1da and the metaproteomics data. The MPE between the ADM1da and the protein data was calculated with the monthly averaged relative COD values of the ADM1da and the relative protein abundances (sampling was once a month) of the MAGs in each group. Additionally, a Spearman correlation was calculated with the ranks of the relative protein abundance of the MAGs in each group (sampling was once a month) and the monthly averaged relative COD values of the ADM1da model output (Supplementary Table 6). Afterwards, the median and average absolute deviation were calculated from the MPE and the Spearman correlation.

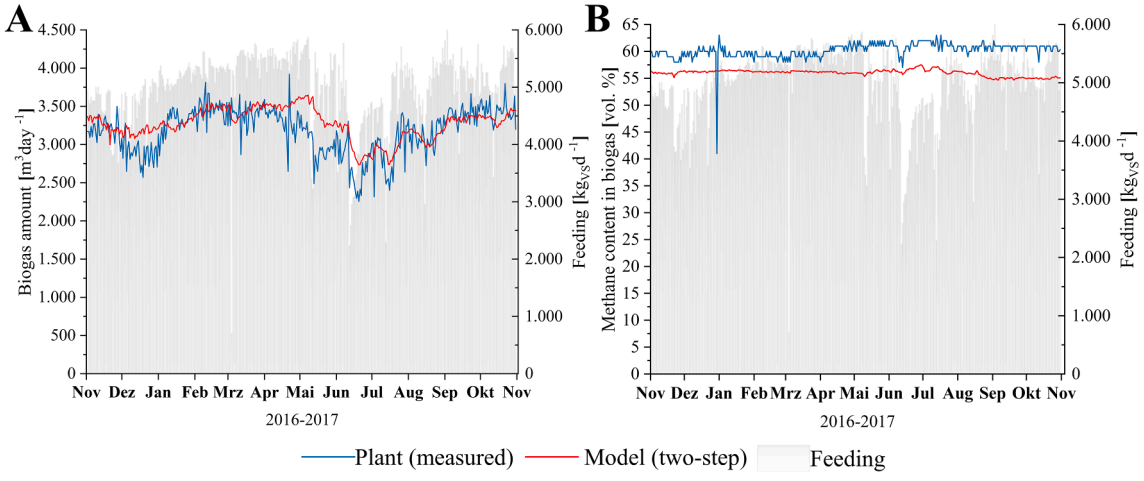

Fig. 4. Comparison of the biogas amount and the methane content of the actual anaerobic digester compared to the ADM1da model. The simulation is based on daily values for feed quantities and monthly measured values for TS content or average values to describe the qualities of the different substrates. **A:** Simulation of the amount of biogas produced from the two-step AD-P with an open hydrolysis fermenter. **B:** Simulation of the methane content produced from the two-step AD-P with an open hydrolysis fermenter.

Table 1

High-quality MAG assignment to the seven trophic groups of the ADM1da based on protein data. MAGs were grouped based on four different rules (Table 2). If the MAG has been assigned to the group, the box is filled with the corresponding color of the group. If no assignment has been made, the box is empty. MAGs that fit into multiple groups based on their identified proteins were assigned to all relevant groups by dividing their abundance equally. The abundance of each MAGs is indicated in yellow for <1 %, orange for >1 %, and red for >5 %.

	MAG_ID	2	7	11	13	17	21	27	34	40	43	57	66	67	69	78	87	90	98	99	106
<1% >1% >5%	Abundance HF	>5%	<1%	<1%	<1%	>5%	<1%	<1%	<1%	<1%	<1%	<1%	<1%	<1%	<1%	<1%	<1%	>1%	>1%	<1%	<1%
	Abundance MF	>5%	<1%	<1%	<1%	<1%	<1%	<1%	<1%	<1%	<1%	<1%	<1%	<1%	>1%	>1%	<1%	<1%	>1%	<1%	<1%
	Taxonomy	*G Methanothrix*	*C Dethiobacteria*	*F Acutalibacteraceae*	*O Acetivibrionales*	*G Prevotella*	*G Eubacterium_B*	*G Methanobacterium*	*O Oscillospirales*	*unknown*	*S Thermoactinomyces vulgaris*	*G Solobacterium*	*S Syntrophosphaera thermopropionivorans*	*O Bacteroidales*	*S Herbinix luporum*	*F Chitinispirillaceae*	*G Herbinix*	*G Pseudoscardovia*	*F Syntrophomonadaceae*	*P Acidobacteriota*	*P Actinobacteriota*
1) Sugar X_{su}	Literature rule				■	■			■		■	■		■	■		■	■			
	Pathway present rule	■			■	■				■		■	■		■	■	■	■	■		
	Extended pathway rule					■									■			■			
	Fine-tuned pathway rule					■									■			■			
2) Amino acids X_{aa}	Literature rule					■								■							
	Pathway present rule	■			■	■	■			■			■	■	■	■		■	■		
	Extended pathway rule																		■		
	Fine-tuned pathway rule																				
3) Fatty acids X_{fa}	Literature rule						■		■										■		
	Pathway present rule					■									■			■			
	Extended pathway rule																	■			
	Fine-tuned pathway rule																				
4) Propionate X_{pro}	Literature rule												■								
	Pathway present rule																		■		
	Extended pathway rule																		■		
	Fine-tuned pathway rule																				
5) Valerate/Butyrate X_{c4}	Literature rule																		■		
	Pathway present rule																		■		
	Extended pathway rule																		■		
	Fine-tuned pathway rule																		■		
6) Acetoclastic methanogenesis X_{ac}	Literature rule	■																			
	Pathway present rule	■																			
	Extended pathway rule	■																			
	Fine-tuned pathway rule	■																			
7) Hydrogenotrophic methanogenesis X_{h2}	Literature rule							■													
	Pathway present rule	■						■													
	Extended pathway rule	■						■													
	Fine-tuned pathway rule	■						■													

	MAG_ID	109	117	118	119	120	134	148	150	154	160	168	175	183	184	187	193	195	197	199	215	216	223	226	229	237	245	250	251	255
<1% >1% >5%	Abundance HF	<1%	<1%	<1%	>5%	<1%	<1%	<1%	<1%	<1%	<1%	<1%	<1%	<1%	>1%	<1%	<1%	<1%	<1%	<1%	<1%	<1%	>5%	>5%	<1%	<1%	<1%	<1%	<1%	<1%
	Abundance MF	<1%	>1%	<1%	<1%	<1%	>1%	<1%	<1%	<1%	<1%	<1%	<1%	<1%	<1%	<1%	<1%	<1%	>1%	<1%	<1%	<1%	<1%	>5%	>5%	<1%	<1%	<1%	<1%	<1%
	Taxonomy	*F Acutalibacteraceae*	*C Limnochordia*	*F Salinivirgaceae*	*G Eubacterium_H*	*G Syntrophosphaera*	*C Limnochordia*	*G Ruminiclostridium_B*	*G CAG-791*	*G Eubacterium_H*	*G Mogibacterium*	*S Petrimonas mucosa*	*F Oscillospiraceae*	*O Bacteroidales*	*F Lachnospiraceae*	*O Saccharofermentanales*	*F Dethiobacteraceae*	*unknown*	*O Bacteroidales*	*P Caldatribacteriota*	*G Sedimentibacter*	*F Acutalibacteraceae*	*G Olsenella_B*	*O Bacteroidales*	*F Pelotomaculaceae*	*F Lachnospiraceae*	*G Eubacterium_A*	*O Syntrophomonadales*	*G Methanofastidiosum*	*C Bacilli*
1) Sugar X_{su}	Literature rule	■	■		■			■	■	■		■	■		■	■			■	■		■	■	■		■	■			
	Pathway present rule		■	■	■		■	■	■	■		■	■		■				■	■	■		■	■	■	■				
	Extended pathway rule		■	■	■		■		■	■					■				■				■	■	■	■				
	Fine-tuned pathway rule		■	■	■		■		■	■					■					■			■	■						
2) Amino acids X_{aa}	Literature rule	■			■				■	■			■	■	■					■	■	■		■		■	■			
	Pathway present rule	■			■		■	■	■	■	■				■			■	■	■	■	■	■	■	■	■				
	Extended pathway rule				■				■						■								■		■					
	Fine-tuned pathway rule		■						■											■				■						
3) Fatty acids X_{fa}	Literature rule																		■									■		
	Pathway present rule				■					■									■				■	■	■	■		■		
	Extended pathway rule				■					■									■									■		
	Fine-tuned pathway rule				■					■									■									■		
4) Propionate X_{pro}	Literature rule					■	■																		■					
	Pathway present rule																							■	■				■	
	Extended pathway rule																													
	Fine-tuned pathway rule																								■					
5) Valerate/Butyrate X_{c4}	Literature rule																											■		
	Pathway present rule				■				■	■					■			■	■				■	■				■		
	Extended pathway rule									■																		■		
	Fine-tuned pathway rule																													
6) Acetoclastic methanogenesis X_{ac}	Literature rule																													
	Pathway present rule																				■									
	Extended pathway rule																													
	Fine-tuned pathway rule																													
7) Hydrogenotrophic methanogenesis X_{h2}	Literature rule																												■	
	Pathway present rule																													
	Extended pathway rule																													
	Fine-tuned pathway rule																													

Table 2
Overview of the rules used for grouping the high-quality MAGs into the groups of the ADM1da. PPW: pentose-phosphate pathway.

	Literature rule	Pathway present rule	Extended pathway rule	Fine-tuned pathway rule
1) Acidogenesis from sugar X_{su}	https://doi.org/10.1016/j.biortech.2019.121851, https://doi.org/10.3389/fmicb.2016.00778, https://doi.org/10.3390/ani14131965, https://doi.org/10.1128/AEM.01955-16, https://doi.org/10.1128/AEM.01955-16, https://doi.org/10.1111/1462-2920.13382, DOI: 10.1074/jbc.M404311200, https://doi.org/10.1021/jf900617z, https://doi.org/10.1099/ijs.0.000021, https://doi.org/10.1007/10_2016_67, https://doi.org/10.1016/j.chemosphere.2023.139164, https://doi.org/10.3389/fmicb.2017.01881, https://doi.org/10.1099/ijsem.0.001324, https://doi.org/10.1186/s40168-021-01105-x, https://doi.org/10.1099/ijs.0.063230-0, https://doi.org/10.2172/530632, https://doi.org/10.1007/10_2016_67, https://doi.org/10.3389/fmicb.2024.1441865, https://doi.org/10.1016/j.scitotenv.2022.156073, https://doi.org/10.1006/anae.1998.0179, https://doi.org/10.1186/s13068-015-0271-6, https://doi.org/10.3389/fmicb.2021.645174, https://doi.org/10.1099/ijsem.0.004692, https://doi.org/10.3389/fmicb.2016.00778, https://doi.org/10.1111/1462-2920.13382, https://doi.org/10.1006/anae.1998.0179 https://doi.org/10.1186/s13068-015-0271-6, https://doi.org/10.1099/ijsem.0.000902, https://doi.org/10.3390/microorganisms8122024, https://doi.org/10.1128/mra.00507-20, https://doi.org/10.1016/j.biortech.2022.128170, https://doi.org/10.1128/AEM.01955-16, https://doi.org/10.1016/j.biortech.2019.121851, https://doi.org/10.1007/978-3-319-52669-0_16, https://doi.org/10.1515/biol-2018-0017, https://doi.org/10.3389/fmicb.2020.00867, https://doi.org/10.1111/1462-2920.13382, https://doi.org/10.1101/2023.11.26.568696, https://doi.org/10.1016/j.wroa.2023.100174, https://doi.org/10.2172/530632, https://doi.org/10.1007/10_2016_67, https://doi.org/10.1099/ijsem.0.003469, https://doi.org/10.1111/1462-2920.13382, https://doi.org/10.1099/ijsem.0.001103, https://doi.org/10.1128/AEM.01955-16, https://doi.org/10.1016/j.biortech.2019.121851, https://doi.org/10.1006/anae.1998.0179, https://doi.org/10.1099/ijsem.0.006380	Cleavage cellulose + Cleavage hemicellulose + Cleavage starch + Cleavage other sugars + Transport monosaccharide + Transport oligosaccharide + Starch binding > 0	Transport monosaccharide + Transport oligosaccharide + Starch binding > 0 AND Acetate fermentation + Ethanol fermentation + Lactate fermentation+ Butyrate fermentation + Propionate fermentation > 0	Acetoclastic methanogenesis & Hydrogenotrophic methanogenesis = 0 AND (Formiate fermentation + Hydrogenasen) / (Glycolysis + PPW) < 5 AND Log2((Cleavage of sugars + Transport sugars + Starch binding)/ (Cleavage of proteins + Transport amino acids and peptides) > -2 AND Cleavage of sugars + Transport sugars + Starch binding + Cleavage of proteins + Transport amino acids and peptides > 0.01
2) Acidogenesis from amino acids X_{aa}	https://doi.org/10.3390/ani14131965, https://doi.org/10.1128/AEM.01955-16 https://doi.org/10.1016/j.chemosphere.2023.139164, https://doi.org/10.3389/fmicb.2017.01881, https://doi.org/10.2172/530632, https://doi.org/10.1007/10_2016_67, https://doi.org/10.1006/anae.1998.0179, https://doi.org/10.1186/s13068-015-0271-6, https://doi.org/10.3389/fmicb.2016.00778, https://doi.org/10.1111/1462-2920.13382, https://doi.org/10.1006/anae.1998.0179, https://doi.org/10.1186/s13068-015-0271-6, https://doi.org/10.1128/mra.00507-20, https://doi.org/10.1016/j.biortech.2022.128170, https://doi.org/10.3389/fmicb.2020.593006, https://doi.org/10.1128/AEM.01955-16, https://doi.org/10.1016/j.biortech.2019.121851, https://doi.org/10.1101/2023.11.26.568696, https://doi.org/10.1016/j.wroa.2023.100174, https://doi.org/10.1099/ijsem.0.000878, https://doi.org/10.1099/00207713-52-3-801, https://doi.org/10.2172/530632, https://doi.org/10.1007/10_2016_67, https://doi.org/10.1099/ijsem.0.001103,	Cleavage proteins and peptides + Amino acid metabolism > 0	Transport peptide and amino acid > 0 AND Acetate fermentation + Ethanol fermentation + Lactate fermentation + Butyrate fermentation + Propionate fermentation > 0	Acetoclastic methanogenesis & Hydrogenotrophic methanogenesis = 0 AND (Formiate fermentation + Hydrogenasen) / (Glycolysis + PPW) < 5 AND Log2((Cleavage of sugars + Transport

(*continued on next page*)

Table 2 (*continued*)

	https://doi.org/10.1128/AEM.01955-16, https://doi.org/10.1016/j.biortech.2019.121851, https://doi.org/10.1006/anae.1998.0179, https://doi.org/10.1099/ijsem.0.006380			sugars + Starch binding)/ (Cleavage of proteins + Transport amino acids and peptides) < 2 AND Cleavage of sugars + Transport sugars + Starch binding + Cleavage of proteins + Transport amino acids and peptides > 0.01
3) Acetogenesis from fatty acids X_{fa}	https://doi.org/10.1016/j.biortech.2017.09.103, https://doi.org/10.1111/1462-2920.13382, https://doi.org/10.1128/AEM.01955-16, https://doi.org/10.1111/1462-2920.13382, https://doi.org/10.1111/1462-2920.12576, https://doi.org/10.1264/jsme2.ME16057, https://doi.org/10.3389/fmicb.2020.00867, https://doi.org/10.1111/1462-2920.13382, https://doi.org/10.1111/1462-2920.12576, https://doi.org/10.1264/jsme2.ME16057	Cleavage lipids and long chain fatty acids + Acetate fermentation + Ethanol fermentation + Lactate fermentation >0	Cleavage lipids and long chain fatty acids > 0 AND Acetate fermentation + Ethanol fermentation + Lactate fermentation + Butyrate fermentation + Propionate fermentation > 0	Cleavage lipids and long chain fatty acids > 0.01
4) Acetogenesis from propionate X_{pro}	https://doi.org/10.1111/1462-2920.12576, https://doi.org/10.1264/jsme2.ME16057, https://doi.org/10.1111/1462-2920.12576, https://doi.org/10.1264/jsme2.ME16057	Propionate fermentation > 0	Propionate fermentation/ (Glycolysis + PPW) > 2	(Formiate fermentation + Hydrogenasen) / (Glycolysis + PPW) > 5 AND Propionate fermentation > 0.01 AND TCA > 0.01
5) Acetogenesis from valerate/butyrate X_{c4}	https://doi.org/10.1111/1758-2229.12759, https://doi.org/10.1111/1758-2229.12759, https://doi.org/10.1111/1462-2920.15388, doi: 10.1101/gr.7136508, https://doi.org/10.1099/ijs.0.64925-0	Butyrate fermentation > 0	Butyrate fermentation/ (Glycolysis+ PPW) > 2	(Formiate fermentation + Hydrogenasen) / (Glycolysis + PPW) > 5 AND Butyrate fermentation > 0.01

(*continued on next page*)

Table 2 (*continued*)

6) Acetoclastic methanogenesis X_{ac}	https://doi.org/10.1128/aem.47.4.796-807.1984, https://doi.org/10.1111/j.1574-6968.1992.tb04987.x	Acetoclastic methanogenesis > 0	Superkingdom: *Archaea* AND Acetoclastic methanogenesis > 0	Acetoclastic methanogenesis > 0.01
7) Hydrogenotrophic methanogenesis X_{h2}	doi: 10.1021/acs.est.0c05525, https://doi.org/10.1002/jctb.5246, https://doi.org/10.1002/wer.1357, https://doi.org/10.1021/acs.est.0c01732	Hydrogenotrophic methanogenesis > 0	Superkingdom: *Archaea* AND Hydrogenotrophic methanogenesis > 0	Hydrogenotrophic methanogenesis > 0.01

$$MPE = \frac{100\%}{n} \sum_{t=1}^{n} \frac{m_t - p_t}{p_t}$$

n: number of values t: value number (time) m_t: model values p_t: biomass values from metaproteomics

3. Results and discussion

The ADM1da model was calibrated using operating data and could be adjusted to the process data of the AD-P with measured values for biogas, methane content, and methane production (MPE/quadratic mean error ≤ 12.4 %, Supplementary Note). Table S1 in Supplementary Note shows the changes of model parameters from the default values to calibrate the model. Despite minor deviations, for example, in pH or VFA, the model allowed statements to be made about trophic groups from ADM1, and revealed methane losses due to open hydrolysis (Supplementary Note). Therefore, the model should be sufficiently accurate to enable a valid comparison with the metagenome-centric metaproteomics data.

3.1. The microbial community of the two-step anaerobic digester

A metagenomic-centric metaproteomic investigation was conducted (see for all details (Heyer et al., 2024)), which revealed the microbial dynamics of 262 MAGs. Of these, 49 MAGs had a high quality, which accounted for 52.7 % of the identified spectra in the main fermenter and 54.8 % in the hydrolysis fermenter. It is noteworthy that 9 of these MAGs constituted 47.66 % of the identified spectra in the main fermenter (abundance ≥ 1 %), and 8 MAGs accounted for 48.95 % in the hydrolysis fermenter (abundance ≥ 1 %) (Tables 1 and Fig. 5). This finding suggests that approximately 8 (in the hydrolysis fermenter) to 9 (in the main fermenter) MAGs constitute roughly half of the biomass in this AD-P on average. Fluctuations in process parameters, especially in the hydrolysis fermenter, and seasonal feeding resulted in dynamic changes in the abundance of dominant MAGs throughout the year, as well as shifts in the prevailing biological processes (Fig. 5 and Supplementary Figure 7). For instance, the feeding stop of sugar beets in April (Supplementary Figure 1) had a significant impact on the abundance of specific MAGs such as MAG_229 (family *Pelotomaculaceae*), MAG_223 (genus *Olsenella_B*), and MAG_117 (class *Limnochordia*) (Fig. 5). These seasonal fluctuations could lead to larger deviations when the data is compared with the ADM1da model, especially when very abundant, high-quality MAGs are affected. Feeding also led to the formation of cellulose- and hemicellulose-degrading enzymes dependent on feeding throughout the year, indicating different degradation rates (Supplementary Figures 8 and 9). Unfortunately, no comparison can be made with the model here, as hydrolysis is not a microbial group in the used ADM1da model. Additionally, the metagenomic-centric metaproteomic data reveal evidence of phage dynamics (Supplementary Figure 10). The ADM1da model used does not include terms for phages, so this data cannot be used in this study. The same applies to the identified syntrophic acetate-oxidizing bacteria, lactate-fermenting bacteria, and ethanol-fermenting bacteria. With the mentioned restrictions, the remaining identified high-quality MAGs were classified into the trophic groups of the ADM1da model based on these metaproteome data in order to enable a comparison between the used ADM1da model and the metaproteome data.

3.2. Functional classification of high-quality MAGs in microbial groups of the ADM1 model

The assignment of MAGs to the seven microbial groups in the ADM1da model enabled the linkage of 38 MAGs based on (i) "Literature Rule", 37 MAGs based on (ii) "Pathway Presence Rule", 16 MAGs based on (iii) "Extended Pathway Rule", and 19 MAGs based on (iv) "Fine-Tuned Pathway Rule" (Table 1). This enabled the assignment of between 32 % and 78 % of the MAGs to the trophic groups, thereby facilitating a comparison of the predicted biomass (model output) with the factual community composition (metaproteomics data).

3.3. Comparison of ADM1da predictions with metaproteome data within the seven trophic model groups

The various rules developed were compared with the ADM1da model output, and their performance was compared with each other. The lowest deviation (median of MPE ± average absolute deviation of MPE) to the model output data was achieved with the (ii) "Pathway Presence Rule" (MPE for hydrolysis: 67.22 % ± 41.71 %, MPE for main fermenter: 54.26 % ± 28.73 %), followed by the (iii) "Extended Pathway Rule" (MPE for hydrolysis: 56.21 % ± 77.35 %, MPE for main fermenter: 59.24 % ± 23.39 %). The (iv) "Fine-Tuned Pathway Rule" (MPE for hydrolysis: 61.78 % ± 35.93 %, MPE for main fermenter: 51.27 % ± 96.99 %) and (i) "Literature Rule" (MPE for hydrolysis: 52.50 % ± 1235.67 %, MPE for main fermenter: 50.46 % ± 309.20 %) showed lower accuracy (Fig. 6).

The highest correlation (median of Spearman's rank correlation coefficient ± average absolute deviation of Spearman's rank correlation coefficient) to model was achieved by, iii) "Extended Pathway Rule" (correlation for hydrolysis: 45.45 % ± 28.51 %, correlation for main fermenter: 57.34 % ± 13.96 %), followed by the (iv) "Fine-Tuned Pathway Rule" (correlation for hydrolysis: 45.45 % ± 28.06 %, correlation for main fermenter: 45.45 % ± 16.07 %) and (i) "Literature Rule" (correlation for hydrolysis 42.66 % ± 21.72 %, correlation for main

fermenter: 44.06 % ± 16.98 %) and (ii) "Pathway Presence Rule" (correlation for hydrolysis: 65.03 % ± 17.30 %, correlation for main fermenter: 32.17 % ± 15.07 %) (Fig. 6).

3.4. Evaluation of the mapping and possible explanations for deviations

For the first time, protein abundances of MAGs representing community composition could be compared with the trophic groups of the ADM1da model. For some trophic groups of the ADM1da model, this mapping resulted in correlations of over 90 % and an MPE of <10 %. However, the accuracy of the mapping varies from group to group. Certain rules showed a high agreement with the ADM1da model for certain trophic groups of the ADM1da model, but are less effective for others. Despite refining the mapping rules, our efforts to achieve complete consistency between the ADM1da model and the metaproteome data were unsuccessful. Furthermore, the refinement of the mapping rules resulted in a decline in mapping quality rather than an enhancement. In particular, the "Fine-Tuned Pathway" rule, which was expected to provide the most biologically accurate assignment of MAGs to trophic groups, did not perform as expected. This suggests that more accurate biological classifications do not necessarily lead to better ADM1da model fit. In fact, the best results were obtained with a coarser classification of the MAGs (e.g., "Extended Pathway Rule"). This could indicate that although the ADM1da model represents the main groups of biological activities, but it does not represent the specific ecological niches of each MAG.

The following explanations are possible reasons for the discrepancies between the ADM1da model and the metaprotein data:

(1) The greatest variance was observed in the abundance and dynamics of sugar, amino acid, and fatty acid degraders. Several MAGs, such as MAG_98 (family *Syntrophomonadaceae*) and MAG_154 (genus *Eubacterium_H*), exhibited functions that could have been assigned to multiple groups of ADM1da and did not have just a single function, as the model assumed. Therefore, it was not possible to assign these MAGs to a single group, and they were split equally into up to four trophic groups depending on the rule (Table 1), neglecting the factual proportions of functions. Another problem arose when classifying bacteria into the group of sugar degraders. Some MAGs of those were exclusively involved in monomer degradation (e.g., MAG_117 (class *Limnochordia*) and MAG_229 (family *Pelotomaculaceae*), while a few, e.g., MAG_69 (species *Herbinix luporum*) and MAG_78 (family *Chitinispirillaceae*), have been shown to encode additionally hydrolytic enzymes (Supplementary Figures 8 and 9). Since hydrolysis is not a separate biological group in the ADM1da model, the non-hydrolyzing and hydrolyzing bacteria have been commonly assigned to sugar degradation, neglecting the essential feature of hydrolysis. Another phenomenon was the changed abundance of MAGs, such as MAG_229 (family *Pelotomaculaceae*) and 223 (genus *Olsenella_B*), due to changed feeding with sugar beets (Fig. 5 and Supplementary Figure 1). In the model, there was almost no change in the relative COD of x_{su} in the hydrolysis fermenter (Fig. 6). From a biological standpoint, these alterations in protein abundance are rational because alternative substrates are known to be preferred by other bacteria.

(2) As documented in the literature, *Methanotrix* (MAG_2), which constituted 24 % of the biomass and was the most abundant MAG of this AD-P, is a strictly acetoclastic *archaeon* (Dueholm et al., 2024). However, the expressed proteins suggested that *Methanotrix* was using hydrogenotrophic methanogenesis via direct electron transfer (Heyer et al., 2024; Khesali Aghtaei et al., 2022; Zhou et al., 2023). Consequently, its group assignment showed a significant influence on the observed fluctuations. For example, in „Literature rule", this MAG caused by far the greatest error, because of the strict assignment to the acetoclastic group (Fig. 6).

(3) Despite successfully linking key MAGs representing this AD-P to the trophic groups of the ADM1da, many highly abundant MAGs, such as MAG_78 (1.77 %, family *Chitinispirillaceae*), MAG_113 (2.97 %, class *Limnochordia*), MAG_117 (1.29 %, class *Limnochordia*), and MAG_153 (1.82 %, order *Caldatribacteriales*), were not linked to the ADM1da model. MAG_113 may act as a fermenting bacterium, but its sequence quality was low, as was MAG_153, which might be a giant virus (A32-like ATPase (A32)) (Mavian et al., 2012). MAG_78 and MAG_117 are high-quality MAGs identified as hydrolyzing and syntrophic acetate-oxidizing bacteria. As previously mentioned, these bacteria were not considered for this study due to their absence in the ADM1da model used. However, these should be integrated into the ADM1 model in the future (Basile et al., 2023; Capson-Tojo et al., 2021). In addition, a few other low abundant high-quality MAGs (<1 %) could not be assigned to the trophic groups of the ADM1 model: MAG_7 (class *Dethiobacteria*), MAG_11 (family *Acutalibacteraceae*), MAG_99 (phylum *Acidobacteriota*), MAG_106 (phylum *Actinobacteriota*), MAG_193 (family *Dethiobacteraceae*), and MAG_255 (class *Bacilli*). In this case, the resolution of the data proved insufficient for a clear assignment of these MAGs to the trophic groups of the ADM1 model.

(4) Limited resolution of metagenomics and metaproteomics: Current sequencing and proteomics methods still restrict our ability to fully decipher microbiome complexity. For instance, only 50 % of the biomass was comprised of high-quality MAGs, while 25 % of the biomass could not be assigned to any MAG. However, this limitation will be overcome as sequencing depth continuously improves (Hu et al., 2021; Minich et al., 2025), along with the advent of novel mass spectrometry techniques and DIA-based metaproteomics workflows (Dumas et al., 2024; Gómez-Varela et al., 2023; Xian et al., 2025). Matching this, it was only feasible to calculate the abundance of microbial groups based on the spectral abundance of all proteins in a MAG, rather than focusing on marker proteins like ribosomal proteins (Suh et al., 2005), which could potentially offer better correlation with activity (Starke et al., 2022).

(5) A major problem is the time axis difference between the model and the metaprotein data. While the model uses daily values, only monthly samples were available for this metagenome-centric metaproteome analysis. An interpolation of the metaproteomics data between sampling points was not possible, so comparison between the ADM1da model and the metaproteomics data could only be calculated using monthly averages. Although it was not possible in this study, it would be preferable if daily sampling were feasible, allowing the model and protein data to have the same timescale. Furthermore, the metagenome was sequenced at only one time point, meaning that only the MAGs that were present at that time were included in the metagenome, and only their proteins could be analyzed using metaproteomics. Although the genome of a microorganism is stable over time, unlike its proteome, it cannot be ruled out that other microorganisms were missed at other times. Consequently, their proteins could not be detected in the metaproteome analysis.

3.5. Interface between modeling and metaproteomics

For the first time, an attempt was made to compare the ADM1da model data with metagenome-centric metaprotein data. The most striking discrepancy between the model and metaprotein data was the high dynamics of proteins, while the model often predicted constant COD (Fig. 6). Thus, dynamic protein data could offer an advantage because it is a more sensitive signal for changing process parameters and could represent the abundance of a MAG (Fig. 5) better. Here, the ADM1

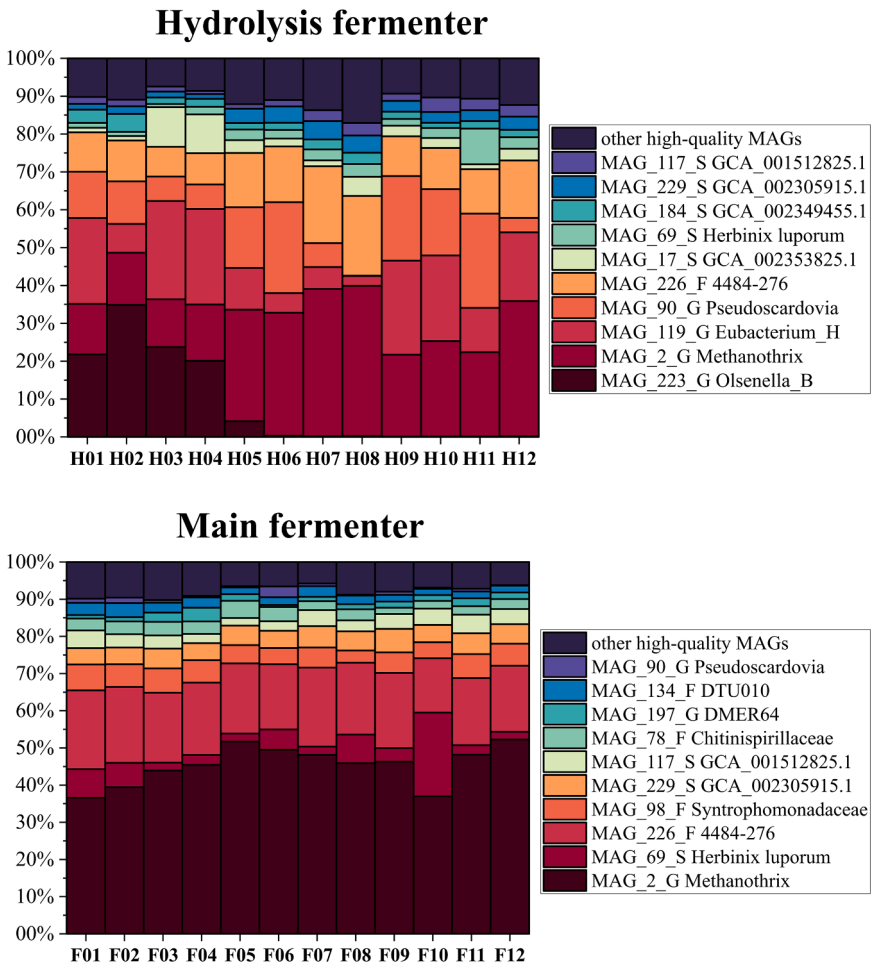

Fig. 5. Dynamics of the top 10 high-quality MAGs in the hydrolysis and main fermenter based on their proteins. The protein abundance of the individual MAGs was averaged across the triplicates and sorted in descending order. The MAGs with the 10 highest protein abundances were displayed in the respective plot. The remaining 39 high-quality MAGs were grouped as "other high-quality MAGs".

model could benefit from the protein information.

However, for follow-up studies, a systematic collection of daily samples from different AD-Ps would be necessary. Combined with corresponding process parameters, it would enable the better correlation of metagenome-centric metaproteomic data with the ADM1da model. Another technical limitation is the incomplete coverage of microbial communities by metagenomic and metaproteomic data. In our proteomic dataset, despite high-resolution metagenomic data, only 50 % of the biomass was assigned to high-quality MAGs, while 25 % of the biomass was not assigned to any MAG. This limited classification of MAGs in metagenomic data could be overcome with increasingly more extensive sequencing and further improvement of genome assembly methods in the future. Furthermore, data-independent acquisition mass spectrometry methods could enable significantly deeper protein resolution and more accurate quantification of low-abundant but functionally relevant proteins (Xian et al., 2025).

In order to use metagenome-centric metaprotein data for modeling, a significant improvement in the strategy for grouping MAGs is required. First, the current grouping was only performed using metaproteomic data at the time of metagenome sequencing. Considering the significant changes in the proteome, classification could be improved by considering time as an essential variable. To implement the approach, automated solutions for grouping, applying machine learning or neural networks should be tested. Second, weighting strategies should be developed to define the extent to which MAGs can be split into more than one group. The present study used the overall abundance of metabolic pathways to assign MAGs into the ADM1da model trophic groups. Further developments should test the abundance of key enzymes for metabolic pathways or ribosomal proteins of key species as more reliable indicators to weight the proportion of MAGs in the groups (Starke et al., 2022; Suh et al., 2005). However, more precise rules showed greater deviations, questioning whether more correlation between the protein data and the model could be reached by more and more sophisticated classification rules or by overdue adaptation of the ADM1 model, integrating recent biological knowledge into the model's differential equations. Metaproteomic data linking functional and phylogenetic data provided sufficient evidence to include new functional groups and respective reactions to ADM1 as previously discussed by other authors (Basile et al., 2023). Most urgent adaptations should consider hydrolysis (Supplementary Figures 8 and 9), additional pathways, such as SAO or ethanol fermentation (Supplementary Figure 7), and (phage-induced) mortality (Supplementary Figure 10). In this study, commercial software implementing ADM1 impeded straightforward access to the model terms for respective modifications. For future model improvements, open-accessible implementations of the ADM1 model should be preferred.

Furthermore, modelling could be improved by analyzing metabolic fluxes using flux balance analysis based on omics data (Basile et al., 2023, 2020; Bernardini et al., 2022; Koch et al., 2016; Lange et al., 2024; Weinrich et al., 2019).

In summary, we would recommend the following steps for the use of metagenome-centric metaproteome data with the ADM1da model:

Hydrolysis fermenter

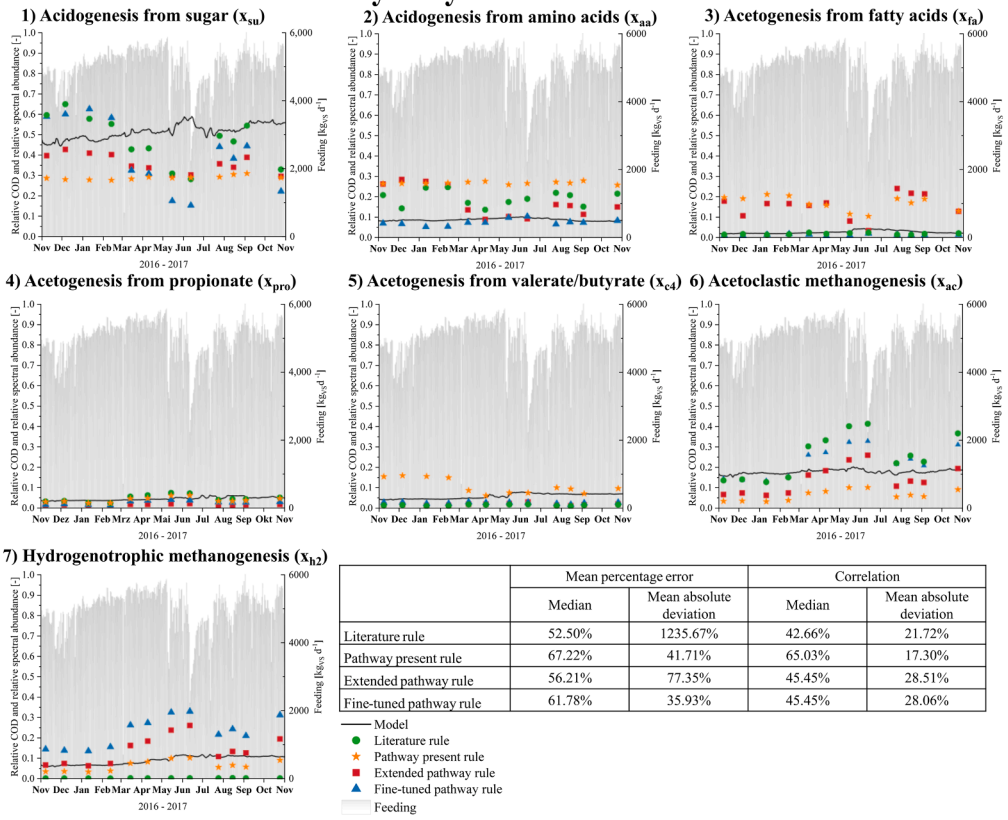

	Mean percentage error		Correlation	
	Median	Mean absolute deviation	Median	Mean absolute deviation
Literature rule	52.50%	1235.67%	42.66%	21.72%
Pathway present rule	67.22%	41.71%	65.03%	17.30%
Extended pathway rule	56.21%	77.35%	45.45%	28.51%
Fine-tuned pathway rule	61.78%	35.93%	45.45%	28.06%

Main fermenter

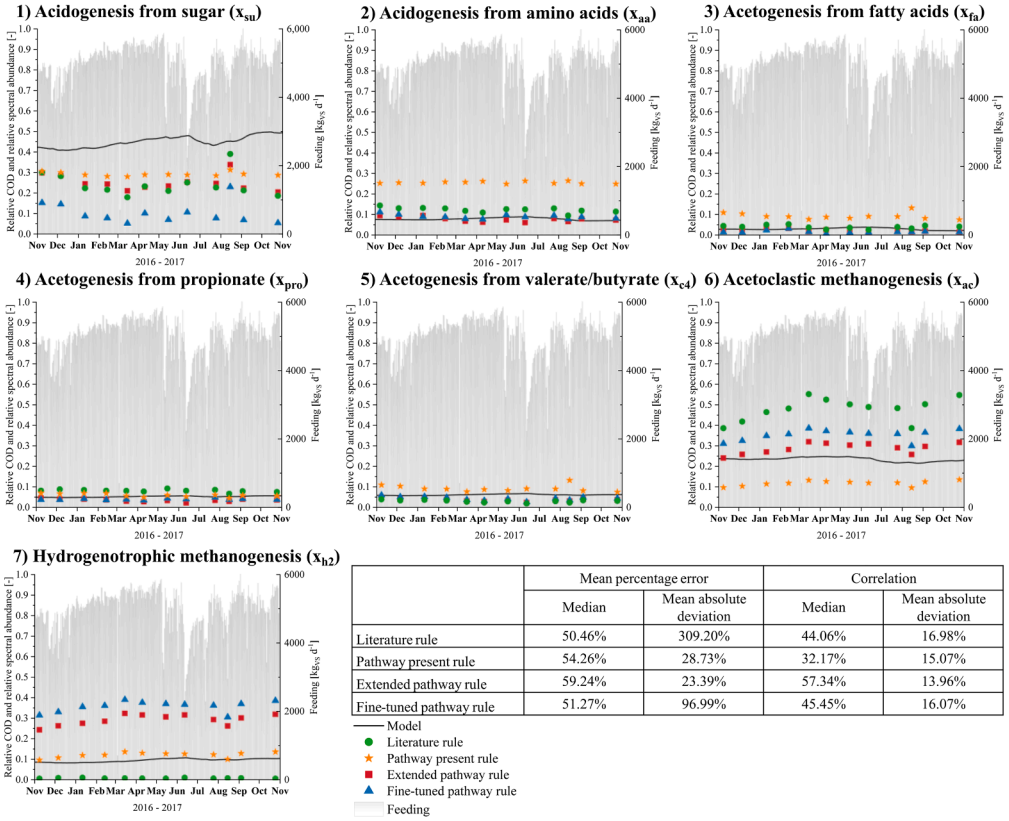

	Mean percentage error		Correlation	
	Median	Mean absolute deviation	Median	Mean absolute deviation
Literature rule	50.46%	309.20%	44.06%	16.98%
Pathway present rule	54.26%	28.73%	32.17%	15.07%
Extended pathway rule	59.24%	23.39%	57.34%	13.96%
Fine-tuned pathway rule	51.27%	96.99%	45.45%	16.07%

(caption on next page)

Fig. 6. Comparison between predicted and measured biomass composition of the seven trophic groups of the ADM1da model. Following the grouping of MAGs into the seven categories defined by the ADM1da model (see Table 1). To allow a direct comparison, the protein abundances of the MAGs in each group were normalized to 100 %. Similarly, the predicted COD values for ADM1da groups were normalized to 100 %. Protein assignments to the microbial groups in ADM1da are based on the association of proteins or genes with high-abundance, high-quality MAGs. The MPE was calculated based on residuals, and the correlation was calculated using Spearman's correlation. For clarity, only the median and mean absolute deviation of the MPE and correlation values across the various rules are shown in this figure. The MPE and correlation values for each microbial group in the ADM1da model, based on each rule applied, are shown in Supplementary Table 6.

- Use deeply sequenced metagenomics and high-resolution metaproteomics data.
- Sample more frequently (daily) for metaproteomics to better match the temporal resolution of ADM1.
- Invest in the development of dynamic weighting strategies for assigning MAGs to model groups based on Kyoto Encyclopedia of Genes and Genomes (KEGG) Orthology (KO) annotations (Kanehisa et al., 2025), abundances of selected key proteins, and completeness of metabolic pathways.
- Expand the model to include additional microbial groups such as hydrolyzing, syntrophic acetate-oxidizing or ethanol-/lactate-fermenting organisms, as well as microbial (phage-induced) mortality (Krysiak-Baltyn et al., 2017).

Implementing suggested improvements in ADM1 shows the potential to minimize the efforts for model calibration, and the dynamics of corrected trophic groups could be used as early indicators for process stability or disturbances.

4. Conclusions

A novel protocol was developed and employed to assign metagenome-centric metaproteomics data to trophic groups included in ADM1. Fluctuations in MAG abundance values over time were significantly greater than fluctuations in predicted ADM1 biomass concentrations. Some deviations were related to difficulties in classifying MAGs into trophic groups of ADM1, since several MAGs performed multiple functions, which was contrary to the model assumption. Furthermore, several functions observed in the metaproteomics data, such as syntrophic acetate oxidizers, hydrolytic bacteria, lactate- and ethanol-fermenting bacteria, and mortality by phages, were not covered by the recent model. These findings underscore the need for data-driven improvement and validation of the model's biological accuracy, even if the ADM1da can adequately represent the process data. In the future, more accurate models considering molecular data could support a deeper understanding of microbial community dynamics in AD-Ps.

Funding

This work was supported by the German Federal Ministry of Food and Agriculture (Grants nos. 22404015 and 22404115 and the German Federal Ministry of Education and Research (de.NBI network project MicroGenUniBi. Grant no. 031L0103). We acknowledge support by the Open Access Publication Fund of Magdeburg University.

Data Availability Statement

Proteome data were stored on PRIDE with the accession number: PXD044302 (http://www.ebi.ac.uk/pride/archive/projects/PXD044302)

Metagenome datasets were stored on Ena under the project number PRJEB39821. The reads were stored under the number accessions ERS15898928 through ERS15898933. The assembled metagenome data were stored under the accession number ERS17165236.

Conflicts of interest

Not applicable.

Declaration of generative AI in scientific writing

ChatGPT and Grammarly were used to improve spelling and expression.

CRediT authorship contribution statement

Patrick Hellwig: Writing – original draft, Visualization, Validation, Methodology, Formal analysis, Data curation, Conceptualization. **Ingolf Seick:** Writing – review & editing, Software, Methodology, Formal analysis, Data curation, Conceptualization. **Nicole Meinusch:** Software, Methodology. **Dirk Benndorf:** Writing – review & editing, Supervision, Methodology. **Jürgen Wiese:** Writing – review & editing, Supervision, Resources. **Udo Reichl:** Writing – review & editing, Supervision, Resources, Funding acquisition. **Robert Heyer:** Writing – review & editing, Supervision, Project administration, Conceptualization.

Declaration of competing interest

The authors declare that they have no known competing financial interests or personal relationships that could have appeared to influence the work reported in this paper.

Acknowledgement

None

Supplementary materials

Supplementary material associated with this article can be found, in the online version, at doi:10.1016/j.watres.2025.125272.

Data availability

Data will be made available on request.

References

Akinsola, O.A., Dahunsi, S.O., Odekanle, E.L., 2025. Metagenomic study of food waste anaerobic digestion. Microbiol. Spectr., e0208725 https://doi.org/10.1128/spectrum.02087-25.

Alex, J., Ogurek, M., Schütze, M., 2013. A novel simulation platform to test WWTP control options.: 11th IWA conference on instrumentation control and automation, 18.-20. September 2013, Narbonne (France).

Azman, S., Khadem, A.F., van Lier, J.B., Zeeman, G., Plugge, C.M., 2015. Presence and role of Anaerobic hydrolytic microbes in conversion of lignocellulosic biomass for biogas production. Crit. Rev. Environ. Sci. Technol. 45, 2523–2564. https://doi.org/10.1080/10643389.2015.1053727.

Basile, A., Campanaro, S., Kovalovszki, A., Zampieri, G., Rossi, A., Angelidaki, I., Valle, G., Treu, L., 2020. Revealing metabolic mechanisms of interaction in the anaerobic digestion microbiome by flux balance analysis. Metab. Eng. 62, 138–149. https://doi.org/10.1016/j.ymben.2020.08.013.

Basile, A., Zampieri, G., Kovalovszki, A., Karkaria, B., Treu, L., Patil, K.R., Campanaro, S., 2023. Modelling of microbial interactions in anaerobic digestion: from black to glass box. Curr. Opin. Microbiol. 75, 102363. https://doi.org/10.1016/j.mib.2023.102363.

Batstone, D.J., Keller, J., Angelidaki, I., Kalyuzhnyi, S.V., Pavlostathis, S.G., Rozzi, A., Sanders, W.T.M., Siegrist, H., Vavilin, V.A., 2002. The IWA anaerobic digestion model no 1 (ADM1). Water Sci. Tech. 45, 65–73.

Bensmann, A., Hanke-Rauschenbach, R., Heyer, R., Kohrs, F., Benndorf, D., Kausmann, R., Plöchl, M., Heiermann, M., Reichl, U., Sundmacher, K., 2016. Diagnostic concept for dynamically operated biogas production plants. Renew. Energy 96, 479–489. https://doi.org/10.1016/j.renene.2016.04.098.

Bensmann, A., Hanke-Rauschenbach, R., Heyer, R., Kohrs, F., Benndorf, D., Reichl, U., Sundmacher, K., 2014. Biological methanation of hydrogen within biogas plants: a

model-based feasibility study. Appl. Energy 134, 413–425. https://doi.org/10.1016/j.apenergy.2014.08.047.
Bensmann, A., Hanke-Rauschenbach, R., Sundmacher, K., 2013. Reactor configurations for biogas plants – a model based analysis. Chem. Eng. Sci. 104, 413–426. https://doi.org/10.1016/j.ces.2013.09.025.
Bernardini, N.de, Basile, A., Zampieri, G., Kovalovszki, A., Diaz, Diego, de, B., Offer, E., Wongfaed, N., Angelidaki, I., Kougias, P.G., Campanaro, S., Treu, L., 2022. Integrating metagenomic binning with flux balance analysis to unravel syntrophies in anaerobic CO2 methanation. Microbiome 10, 117. https://doi.org/10.1186/s40168-022-01311-1.
Blumensaat, F., Keller, J., 2005. Modelling of two-stage anaerobic digestion using the IWA Anaerobic Digestion Model No. 1 (ADM1). Water. Res. 39, 171–183. https://doi.org/10.1016/j.watres.2004.07.024.
Bowers, R.M., Kyrpides, N.C., Stepanauskas, R., Harmon-Smith, M., Doud, D., Reddy, T. B.K., Schulz, F., Jarett, J., Rivers, A.R., Eloe-Fadrosh, E.A., Tringe, S.G., Ivanova, N. N., Copeland, A., Clum, A., Becraft, E.D., Malmstrom, R.R., Birren, B., Podar, M., Bork, P., Weinstock, G.M., Garrity, G.M., Dodsworth, J.A., Yooseph, S., Sutton, G., Glöckner, F.O., Gilbert, J.A., Nelson, W.C., Hallam, S.J., Jungbluth, S.P., Ettema, T.J. G., Tighe, S., Konstantinidis, K.T., Liu, W.-T., Baker, B.J., Rattei, T., Eisen, J.A., Hedlund, B., McMahon, K.D., Fierer, N., Knight, R., Finn, R., Cochrane, G., Karsch-Mizrachi, I., Tyson, G.W., Rinke, C., Lapidus, A., Meyer, F., Yilmaz, P., Parks, D.H., Eren, A.M., Schriml, L., Banfield, J.F., Hugenholtz, P., Woyke, T., 2017. Minimum information about a single amplified genome (MISAG) and a metagenome-assembled genome (MIMAG) of bacteria and archaea. Nat. Biotechnol. 35, 725–731. https://doi.org/10.1038/nbt.3893.
Campanaro, S., Treu, L., Rodriguez-R, L.M., et al., 2020. New insights from the biogas microbiome by comprehensive genome-resolved metagenomics of nearly 1600 species originating from multiple anaerobic digesters. Biotech. Biofuels 13, 25. https://doi.org/10.1186/s13068-020-01679-y.
Capson-Tojo, G., Astals, S., Robles, Á., 2021. Considering syntrophic acetate oxidation and ionic strength improves the performance of models for food waste anaerobic digestion. Bioresour. Technol. 341, 125802. https://doi.org/10.1016/j.biortech.2021.125802.
Cirne, D.G., Lehtomäki, A., Björnsson, L., Blackall, L.L., 2007. Hydrolysis and microbial community analyses in two-stage anaerobic digestion of energy crops. J. Appl. Microbiol. 103, 516–527. https://doi.org/10.1111/j.1365-2672.2006.03270.x.
Contois, D.E., 1959. Kinetics of bacterial growth: relationship between population density and specific growth rate of continuous cultures. J. Gen. Microbiol. 21, 40–50. https://doi.org/10.1099/00221287-21-1-40.
Detman, A., Mielecki, D., Pleśniak, Ł., Bucha, M., Janiga, M., Matyasik, I., Chojnacka, A., Jędrysek, M.-O., Błaszczyk, M.K., Sikora, A., 2018. Methane-yielding microbial communities processing lactate-rich substrates: a piece of the anaerobic digestion puzzle. Biotechnol. Biofuels. 11, 116. https://doi.org/10.1186/s13068-018-1106-z.
Du, B., Wang, Y., Wu, G., 2025. Ethanol metabolism in anaerobic digestion systems for better renewable energy recovery from waste feedstocks. Bioresour. Technol. 435, 132862. https://doi.org/10.1016/j.biortech.2025.132862.
Dueholm, M.K.D., Andersen, K.S., Korntved, A.-K.C., Rudkjøbing, V., Alves, M., Bajón-Fernández, Y., Batstone, D., Butler, C., Cruz, M.C., Davidsson, Å., Erijman, L., Holliger, C., Koch, K., Kreuzinger, N., Lee, C., Lyberatos, G., Mutnuri, S., O'Flaherty, V., Oleskowicz-Popiel, P., Pokorna, D., Rajal, V., Recktenwald, M., Rodríguez, J., Saikaly, P.E., Tooker, N., Vierheilig, J., Vrieze, J.de, Wurzbacher, C., Nielsen, P.H., 2024. MiDAS 5: global diversity of bacteria and archaea in anaerobic digesters. Nat. Commun. 15, 5361. https://doi.org/10.1038/s41467-024-49641-y.
Dumas, T., Martinez Pinna, R., Lozano, C., Radau, S., Pible, O., Grenga, L., Armengaud, J., 2024. The astounding exhaustiveness and speed of the Astral mass analyzer for highly complex samples is a quantum leap in the functional analysis of microbiomes. Microbiome 12, 46. https://doi.org/10.1186/s40168-024-01766-4.
Dyksma, S., Jansen, L., Gallert, C., 2020. Syntrophic acetate oxidation replaces acetoclastic methanogenesis during thermophilic digestion of biowaste. Microbiome 8, 105. https://doi.org/10.1186/s40168-020-00862-5.
Feng, D., Guo, X., Lin, R., Xia, A., Huang, Y., Liao, Q., Zhu, X., Zhu, X., Murphy, J.D., 2021. How can ethanol enhance direct interspecies electron transfer in anaerobic digestion? Biotechnol. Adv. 52, 107812. https://doi.org/10.1016/j.biotechadv.2021.107812.
Gómez-Varela, D., Xian, F., Grundtner, S., Sondermann, J.R., Carta, G., Schmidt, M., 2023. Increasing taxonomic and functional characterization of host-microbiome interactions by DIA-PASEF metaproteomics. Front. Microbiol. 14, 1258703. https://doi.org/10.3389/fmicb.2023.1258703.
Harirchi, S., Wainaina, S., Sar, T., Nojoumi, S.A., Parchami, M., Parchami, M., Varjani, S., Khanal, S.K., Wong, J., Awasthi, M.K., Taherzadeh, M.J., 2022. Microbiological insights into anaerobic digestion for biogas, hydrogen or volatile fatty acids (VFAs): a review. Bioengineered. 13, 6521–6557. https://doi.org/10.1080/21655979.2022.2035986.
Hassa, J., Tubbesing, T.J., Maus, I., Heyer, R., Benndorf, D., Effenberger, M., Henke, C., Osterholz, B., Beckstette, M., Pühler, A., Sczyrba, A., Schlüter, A., 2023. Uncovering microbiome adaptations in a full-scale biogas plant: insights from MAG-centric metagenomics and metaproteomics. Microorganisms 11. https://doi.org/10.3390/microorganisms11102412.
Heyer, R., Benndorf, D., Kohrs, F., Vrieze, J.de, Boon, N., Hoffmann, M., Rapp, E., Schlüter, A., Sczyrba, A., Reichl, U., 2016. Proteotyping of biogas plant microbiomes separates biogas plants according to process temperature and reactor type. Biotechnol. Biofuels. 9, 155. https://doi.org/10.1186/s13068-016-0572-4.
Heyer, R., Hellwig, P., Maus, I., Walke, D., Schlüter, A., Hassa, J., Sczyrba, A., Tubbesing, T., Klocke, M., Mächtig, T., Schallert, K., Seick, I., Reichl, U., Benndorf, D., 2024. Breakdown of hardly degradable carbohydrates (lignocellulose) in a two-stage anaerobic digestion plant is favored in the main fermenter. Water. Res. 250, 121020. https://doi.org/10.1016/j.watres.2023.121020.
Heyer, R., Kohrs, F., Reichl, U., Benndorf, D., 2015. Metaproteomics of complex microbial communities in biogas plants. Microb. Biotechnol. 8, 749–763. https://doi.org/10.1111/1751-7915.12276.
Heyer, R., Schallert, K., Büdel, A., Zoun, R., Dorl, S., Behne, A., Kohrs, F., Püttker, S., Siewert, C., Muth, T., Saake, G., Reichl, U., Benndorf, D., 2019a. A robust and universal metaproteomics workflow for research studies and routine diagnostics within 24 h using phenol extraction, FASP digest, and the MetaProteomeAnalyzer. Front. Microbiol. 10, 1883. https://doi.org/10.3389/fmicb.2019.01883.
Heyer, R., Schallert, K., Siewert, C., Kohrs, F., Greve, J., Maus, I., Klang, J., Klocke, M., Heiermann, M., Hoffmann, M., Püttker, S., Calusinska, M., Zoun, R., Saake, G., Benndorf, D., Reichl, U., 2019b. Metaproteome analysis reveals that syntrophy, competition, and phage-host interaction shape microbial communities in biogas plants. Microbiome 7, 69. https://doi.org/10.1186/s40168-019-0673-y.
Heyer, R., Wolf, M., Benndorf, D., Uzzau, S., Seifert, J., Grenga, L., Pabst, M., Schmitt, H., Mesuere, B., van den Bossche, T., Haange, S.-B., Jehmlich, N., Di Luca, M., Ferrer, M., Serrano-Villar, S., Armengaud, J., Bode, H.B., Hellwig, P., Masselot, C.R., Léonard, R., Wilmes, P., 2025. Metaproteomics in the one Health framework for unraveling microbial effectors in microbiomes. Microbiome 13. https://doi.org/10.1186/s40168-025-02119-5.
Hu, T., Chitnis, N., Monos, D., Dinh, A., 2021. Next-generation sequencing technologies: an overview. Hum. Immunol. 82, 801–811. https://doi.org/10.1016/j.humimm.2021.02.012.
ifak GmbH, 2021. Simba#Biogas.
Kanehisa, M., Furumichi, M., Sato, Y., Matsuura, Y., Ishiguro-Watanabe, M., 2025. KEGG: biological systems database as a model of the real world. Nucleic. Acids. Res. 53, D672–D677. https://doi.org/10.1093/nar/gkae909.
Karlsson, J., 2017. Modeling and simulation of existing biogas plants with SIMBA# Biogas.
Khesali Aghtaei, H., Püttker, S., Maus, I., Heyer, R., Huang, L., Sczyrba, A., Reichl, U., Benndorf, D., 2022. Adaptation of a microbial community to demand-oriented biological methanation. Biotechnol. Biofuels. Bioprod. 15, 125. https://doi.org/10.1186/s13068-022-02207-w.
Koch, S., Benndorf, D., Fronk, K., Reichl, U., Klamt, S., 2016. Predicting compositions of microbial communities from stoichiometric models with applications for the biogas process. Biotechnol. Biofuels. 9, 17. https://doi.org/10.1186/s13068-016-0429-x.
Krysiak-Baltyn, K., Martin, G.J., Stickland, A.D., Scales, P.J., Gras, S.L., 2017. Simulation of phage dynamics in multi-reactor models of complex wastewater treatment systems. Biochem. Eng. J. 122, 91–102. https://doi.org/10.1016/j.bej.2016.10.011.
Lange, E., Kranert, L., Krüger, J., Benndorf, D., Heyer, R., 2024. Microbiome modeling: a beginner's guide. Front. Microbiol. 15, 1368377. https://doi.org/10.3389/fmicb.2024.1368377.
Maus, I., Klocke, M., Derenkó, J., Stolze, Y., Beckstette, M., Jost, C., Wibberg, D., Blom, J., Henke, C., Willenbücher, K., Rumming, M., Rademacher, A., Pühler, A., Sczyrba, A., Schlüter, A., 2020. Impact of process temperature and organic loading rate on cellulolytic /hydrolytic biofilm microbiomes during biomethanation of ryegrass silage revealed by genome-centered metagenomics and metatranscriptomics. Environ. Microbiome 15, 7. https://doi.org/10.1186/s40793-020-00354-x.
Maus, I., Koeck, D.E., Cibis, K.G., Hahnke, S., Kim, Y.S., Langer, T., Kreubel, J., Erhard, M., Bremges, A., Off, S., Stolze, Y., Jaenicke, S., Goesmann, A., Sczyrba, A., Scherer, P., König, H., Schwarz, W.H., Zverlov, V.V., Liebl, W., Pühler, A., Schlüter, A., Klocke, M., 2016. Unraveling the microbiome of a thermophilic biogas plant by metagenome and metatranscriptome analysis complemented by characterization of bacterial and archaeal isolates. Biotechnol. Biofuels. 9, 171. https://doi.org/10.1186/s13068-016-0581-3.
Mavian, C., López-Bueno, A., Balseiro, A., Casais, R., Alcamí, A., Alejo, A., 2012. The genome sequence of the emerging common midwife toad virus identifies an evolutionary intermediate within ranaviruses. J. Virol. 86, 3617–3625. https://doi.org/10.1128/JVI.07108-11.
Meinusch, N., Kramer, S., Körner, O., Wiese, J., Seick, I., Beblek, A., Berges, R., Illenberger, B., Illenberger, M., Uebbing, J., Wolf, M., Saake, G., Benndorf, D., Reichl, U., Heyer, R., 2021. Integrated cycles for urban biomass as a strategy to promote a CO2-neutral society—A feasibility study. Sustainability. 13, 9505. https://doi.org/10.3390/su13179505.
Minich, J.J., Allsing, N., Din, M.O., Tisza, M.J., Maleta, K., McDonald, D., Hartwick, N., Mamerto, A., Brennan, C., Hansen, L., Shaffer, J., Murray, E.R., Duong, T., Knight, R., Stephenson, K., Manary, M.J., Michael, T.P., 2025. Culture-independent meta-pangenomics enabled by long-read metagenomics reveals associations with pediatric undernutrition. Cell. https://doi.org/10.1016/j.cell.2025.08.020.
Mo, R., Guo, W., Batstone, D., Makinia, J., Li, Y., 2023. Modifications to the anaerobic digestion model no. 1 (ADM1) for enhanced understanding and application of the anaerobic treatment processes - A comprehensive review. Water. Res. 244, 120504. https://doi.org/10.1016/j.watres.2023.120504.
Moestedt, J., Müller, B., Nagavara Nagaraj, Y., Schnürer, A., 2020. Acetate and lactate production during two-stage Anaerobic digestion of food waste driven by Lactobacillus and aeriscardovia. Front. Energy Res. 8, 105. https://doi.org/10.3389/fenrg.2020.00105.
Mosbæk, F., Kjeldal, H., Mulat, D.G., Albertsen, M., Ward, A.J., Feilberg, A., Nielsen, J.L., 2016. Identification of syntrophic acetate-oxidizing bacteria in anaerobic digesters by combined protein-based stable isotope probing and metagenomics. ISMe J. 10, 2405–2418. https://doi.org/10.1038/ismej.2016.39.
Normak, A., Suurpere, J., Suitso, I., Jõgi, E., Kokin, E., Pitk, P., 2015. Improving ADM1 model to simulate anaerobic digestion start-up with inhibition phase based on cattle

slurry. Biomass and Bioenergy 80, 260–266. https://doi.org/10.1016/j.biombioe.2015.05.021.
Ogurek, M., Seick, I., Kujawski, O., Alex, J., 2013. Toward modeling of biogas plants in engineering practice. In: 11th IWA conference on instrumentation control and automation, 18.-20. September 2013, Narbonne, France.
Orellana, E., Davies-Sala, C., Guerrero, L.D., Vardé, I., Altina, M., Lorenzo, M.C., Figuerola, E.L., Pontiggia, R.M., Erijman, L., 2019. Microbiome network analysis of co-occurrence patterns in anaerobic co-digestion of sewage sludge and food waste. Water Sci. Tech. 79, 1956–1965. https://doi.org/10.2166/wst.2019.194.
Pipyn, P., Verstraete, W., 1981. Lactate and ethanol as intermediates in two-phase anaerobic digestion. Biotech. Bioeng. 23, 1145–1154. https://doi.org/10.1002/bit.260230521.
Rademacher, A., Zakrzewski, M., Schlüter, A., Schönberg, M., Szczepanowski, R., Goesmann, A., Pühler, A., Klocke, M., 2012. Characterization of microbial biofilms in a thermophilic biogas system by high-throughput metagenome sequencing. FEMS. Microbiol. Ecol. 79, 785–799. https://doi.org/10.1111/j.1574-6941.2011.01265.x.
Rivera-Salvador, V., López-Cruz, I.L., Espinosa-Solares, T., Aranda-Barradas, J.S., Huber, D.H., Sharma, D., Toledo, J.U., 2014. Application of Anaerobic Digestion Model No. 1 to describe the syntrophic acetate oxidation of poultry litter in thermophilic anaerobic digestion. Bioresour. Technol. 167, 495–502. https://doi.org/10.1016/j.biortech.2014.06.008.
Rojas, C., Uhlenhut, F., Schlaak, M., Borchert, A., Steinigeweg, S., 2011. Simulation of the Anaerobic process for the biogas production. Chemie Ingenieur Technik 83, 306–321. https://doi.org/10.1002/cite.201000100.
Rossi, A., Morlino, M.S., Gaspari, M., Basile, A., Kougias, P., Treu, L., Campanaro, S., 2022. Analysis of the anaerobic digestion metagenome under environmental stresses stimulating prophage induction. Microbiome 10, 125. https://doi.org/10.1186/s40168-022-01316-w.
Satpathy, P., Biernacki, P., Uhlenhut, F., Cypionka, H., Steinigeweg, S., 2016. Modelling anaerobic digestion in a biogas reactor: ADM1 model development with lactate as an intermediate (Part I). J. Environ. Sci. Health a Tox. Hazard. Subst. Environ. Eng. 51, 1216–1225. https://doi.org/10.1080/10934529.2016.1212558.
Seick, I., Vergara-Araya, M., Wiese, J., 2023. Model-based analysis to increase the substrate efficiency of a biogas plant. Chem. Eng. Technol. 46, 511–521. https://doi.org/10.1002/ceat.202100370.
Sikora, A., Detman, A., Mielecki, D., Chojnacka, A., Błaszczyk, M., 2019. Searching for metabolic pathways of Anaerobic digestion: a useful list of the key enzymes, in: Banu, J.R. (Ed.), Anaerobic Digestion. IntechOpen, Erscheinungsort nicht ermittelbar.
Starke, R., Fiore-Donno, A.M., White, R.A., Parente Fernandes, M.L., Martinović, T., Bastida, F., Delgado-Baquerizo, M., Jehmlich, N., 2022. Biomarker metaproteomics for relative taxa abundances across soil organisms. Soil Bio. Biochem. 175, 108861. https://doi.org/10.1016/j.soilbio.2022.108861.
Suh, M.-J., Hamburg, D.-M., Gregory, S.T., Dahlberg, A.E., Limbach, P.A., 2005. Extending ribosomal protein identifications to unsequenced bacterial strains using matrix-assisted laser desorption/ionization mass spectrometry. Proteomics. 5, 4818–4831. https://doi.org/10.1002/pmic.200402111.
Vrieze, J.de, Saunders, A.M., He, Y., Fang, J., Nielsen, P.H., Verstraete, W., Boon, N., 2015. Ammonia and temperature determine potential clustering in the anaerobic digestion microbiome. Water. Res. 75, 312–323. https://doi.org/10.1016/j.watres.2015.02.025.
Walke, D., Schallert, K., Ramesh, P., Benndorf, D., Lange, E., Reichl, U., Heyer, R., 2021. MPA_Pathway_Tool: user-friendly, automatic assignment of microbial community data on metabolic pathways. Int. J. Mol. Sci. 22. https://doi.org/10.3390/ijms222010992.
Wang, X., Liu, Y., Han, X., Song, H., Li, Q., Chen, M., Li, X., Zhang, D., 2026. Effect and mechanism of lactic acid on anaerobic digestion of acidified food waste. Renew. Energy 256, 124091. https://doi.org/10.1016/j.renene.2025.124091.
Wang, Z.-W., Li, Y., 2014. A theoretical derivation of the Contois equation for kinetic modeling of the microbial degradation of insoluble substrates. Biochem. Eng. J. 82, 134–138. https://doi.org/10.1016/j.bej.2013.11.002.
Weinrich, S., Koch, S., Bonk, F., Popp, D., Benndorf, D., Klamt, S., Centler, F., 2019. Augmenting biogas process modeling by resolving intracellular metabolic activity. Front. Microbiol. 10, 1095. https://doi.org/10.3389/fmicb.2019.01095.
Xian, F., Brenek, M., Krisp, C., Urbauer, E., Ravi Kumar, R.K., Aguanno, D., Srikumar, T., Liu, Q., Barry, A.M., Ma, B., Krieger, J., Haller, D., Schmidt, M., Gómez-Varela, D., 2025. Ultra-sensitive metaproteomics redefines the dark metaproteome, uncovering host-microbiome interactions and drug targets in intestinal diseases. Nat. Commun. 16, 6644. https://doi.org/10.1038/s41467-025-61977-7.
Yang, B., Wang, C., Zhao, X., Liu, J., Yin, F., Liang, C., Wu, K., Liu, J., Yang, H., Zhang, W., 2022. Effects of environmental factors on low temperature anaerobic digestion of pig manure. Environ. Res. Commun. 4, 125006. https://doi.org/10.1088/2515-7620/aca647.
Zhang, C., Su, H., Baeyens, J., Tan, T., 2014. Reviewing the anaerobic digestion of food waste for biogas production. Renew. Sustain. Energy Rev. 38, 383–392. https://doi.org/10.1016/j.rser.2014.05.038.
Zhou, J., Smith, J.A., Li, M., Holmes, D.E., 2023. Methane production by Methanothrix thermoacetophila via direct interspecies electron transfer with Geobacter metallireducens. MBio 14, e0036023. https://doi.org/10.1128/mbio.00360-23.